



**Politecnico
di Torino**

POLITECNICO DI TORINO

Master of Science in Automotive Engineering

Academic Year 2021/22

**Modelling of a BEV thermal management
system and development of its control
strategy in GT-SUITE**

Academic supervisors

Prof. Federico Millo

Prof. Luciano Rolando

Company supervisor

Eduardo Graziano

Candidate

Giovanni Di Grezia

July 2022

IMPORTANT NOTICE

This document contains information which is not intended for publication. All rights of the thesis are owned by POWERTECH Engineering S.r.l. and the contents cannot be published without a written authorization by the already-mentioned company.

PREMESSA

Questo documento contiene informazioni che non sono destinate alla pubblicazione. Tutti i diritti della tesi sono di proprietà di POWERTECH Engineering S.r.l. e non possono esserne diffusi i contenuti senza un'autorizzazione scritta da parte della suddetta azienda.

Abstract

The following master degree thesis has been developed internally at POWERTECH Engineering S.r.l., whose main expertise involves 1D and 3D CFD simulations and SiL/HiL Real-Time modeling.

The main purpose of the project has been about modeling a complete thermal management system of a generic Battery Electric Vehicle (*BEV*), including the main coolant circuit, the Heating and Ventilation Air Conditioning (*HVAC*) refrigerant circuit, the underhood air circuit and the cabin air circuit. Particular attention has been paid to the calibration of the HVAC controls acting on the compressor speed and on the electrovalves flow area, in order to reach the targets in terms of superheat at the compressor inlet and in terms of temperature at the evaporator/chiller outlets, depending on the configuration.

The model built can be employed as a useful tool to perform multi-purpose tests. This thesis wants to prove this statement by providing three possible applications: evaluation of critical operating conditions, dimensioning on HVAC circuit components and selection of the best methodology to heat-up the cabin when requested, exploring the impact that different solutions can have on the battery energy consumption.

The modeling activity and the necessary validation have been developed on GT-SUITE, an industry-leading 1D simulation software capable of providing tools to easily integrate different models and to test them accurately and with high real-world systems fidelity.

Even if the model has been built with the aim of being representative of real-world applications, it takes into account the most common solutions adopted by automotive manufacturers. As a consequence, the provided results are qualitatively accurate and representative of a BEV vehicle platform, although not directly correlated to a specific real vehicle.

Sommario

Il lavoro di tesi presentato di seguito è stato sviluppato in collaborazione con POWERTECH Engineering S.r.l, un'azienda che si occupa principalmente di simulazione 1D, 3D CFD e di Real-Time modeling per applicazioni SiL/HiL.

L'obiettivo principale del progetto ha riguardato la costruzione di un modello di thermal management di un Battery Electric Vehicle (*BEV*) generico, integrando il circuito di raffreddamento principale, il circuito refrigerante (Heating and Ventilation Air Conditioning, *HVAC*), il circuito aria del sottocofano e dell'abitacolo. Impegno particolare è stato profuso nella calibrazione dei controlli sulla velocità del compressore e sull'area delle elettrovalvole nel circuito di HVAC, in modo da poter raggiungere i target in termini di surriscaldamento all'ingresso compressore e in termini di temperature in uscita evaporatore/chiller a seconda della configurazione.

Il modello può essere utilizzato come strumento per eseguire test con diversi obiettivi. La tesi è volta a dare una dimostrazione di come poter applicare il modello, fornendo esempi di individuazione delle condizioni operative più critiche, di dimensionamento dei componenti del circuito HVAC e di selezione della miglior modalità di riscaldamento dell'abitacolo, tenendo in considerazione l'impatto che diverse soluzioni hanno sul consumo dell'energia della batteria.

L'attività di modellazione e di validazione è stata sviluppata su GT-SUITE, un software di simulazione 1D leader nel settore industriale capace di fornire strumenti utili per integrare e testare diversi modelli con elevata precisione e fedeltà ai sistemi reali.

Nonostante il modello sia stato costruito con l'obiettivo di essere il più rappresentativo possibile di applicazioni reali, è frutto delle soluzioni comuni utilizzate dai principali costruttori di veicoli. Di conseguenza, fornisce risultati qualitativamente attendibili e rappresentativi di un veicolo BEV, anche se non direttamente correlato a un veicolo reale.

Contents

List of Tables	VII
List of Figures	VIII
1 Introduction	1
1.1 Context.....	1
1.2 Thermal Management System	3
1.3 HVAC system	5
1.4 BEV Thermal Management System solutions.....	8
1.4.1 Fiat 500e TMS	8
1.4.2 Tesla Model S (2013) TMS.....	8
1.4.3 Tesla Model Y (2019) / Model S and X (2021) TMS	9
2 1D Software – GT SUITE	11
2.1 Flow solution method	12
2.2 Thermal management system modelling	14
3 Thermal Management System Model	16
3.1 Cooling Circuit	17
3.2 Underhood circuit	20
3.3 HVAC circuit.....	21
3.3.1 Model and layout description.....	22
3.3.2 Compressor controls.....	23
3.3.3 Thermal Expansion Valves controls	25
3.4 Cabin circuit.....	27
3.5 HVAC system sensitivity analysis.....	28
3.5.1 Battery cooling – chiller mode.....	28
3.5.2 Cabin cooling – evaporator mode.....	33
4 Model applications	38
4.1 Critical operational points identification	38
4.2 HVAC components selection.....	44

4.3 Cabin heating strategy to optimize energy consumption.....	47
4.3.1 Energy calculation methodology and results	49
Conclusions	53
Bibliography	54

List of Tables

Table 3.1 Data used to model heat-rejecting components.....	17
Table 3.2 Compressor logic.....	24
Table 3.3 HVAC EV areas logic.....	26
Table 4.1 Targets achievement summary.....	43

List of Figures

Figure 1.1 Global EV market growth	2
Figure 1.2 ICE Thermal Management System	3
Figure 1.3 Operating temperatures for vehicle components.....	4
Figure 1.5b Real vehicle application schematic	5
Figure 1.5a Functional schematic of an AC circuit	5
Figure 1.4 Refrigerant cycle in a p-h diagram.....	6
Figure 1.6 Fiat 500e BEV Thermal Management System	8
Figure 1.7 Tesla Model S Thermal Management System	9
Figure 1.8 Tesla Model Y Thermal Management System	10
Figure 2.1 Components discretization	12
Figure 2.2 Navier-Stokes equations.....	13
Figure 3.1 Thermal Management System Model	16
Figure 3.2 Cooling circuit.....	17
Figure 3.4 Pumps operating map.....	19
Figure 3.5a Underhood circuit subassembly	20
Figure 3.5b Underhood subassembly external connection.....	20
Figure 3.6 Fan working map.....	21
Figure 3.7 HVAC circuit	21
Figure 3.8 AC Compressor working map.....	22
Figure 3.9 Compressor control strategy	23
Figure 3.10 Expansion valves control strategy.....	25
Figure 3.11 Cabin circuit	27
Figure 3.12 Blower working map.....	28
Figure 3.13 HVAC flow path	29
Figure 3.14 Chiller outlet temperatures	30
Figure 3.15 Performance summary of superheat PID	31
Figure 3.16 Superheat PID outputs	31
Figure 3.17 Compressor PID outputs	32
Figure 3.18 HVAC flow path	33
Figure 3.19 Cabin circuit flow path.....	34
Figure 3.20 Evaporator outlet temperatures	35
Figure 3.21 Compressor PID outputs	35
Figure 3.22 Performance summary of superheat PID	36
Figure 3.23 Superheat PID outputs	36

Figure 4.1 Full configuration flow path.....	39
Figure 4.2 Performance summary of superheat PID	40
Figure 4.3 Additional PID performance summary	41
Figure 4.4 Performance summary of compressor PID	42
Figure 4.5 Compressor speeds at 25 °C.....	44
Figure 4.6 Performance summary of compressor PID	45
Figure 4.6 Compressor speed control (BASELINE).....	45
Figure 4.7 Performance summary condenser scaling.....	46
Figure 4.8 Compressor speed control (+30%).....	47
Figure 4.9 Refrigerant flow path	48
Figure 4.10 Integration intervals	50
Figure 4.11 Energy calculation results	51

Chapter 1

Introduction

1.1 Context

In recent years the popularity of Electric Vehicles (*EV*) has been growing constantly. Even if the variations among the market regions are strong, the tendency to a more electrified fleet is global. As a matter of fact, the EV market share has expanded to 8.3% in 2021, starting from 0.2% in 2012 ^[1] (*Figure 1.1*). This is the direct result of two factors coming together: the always improving technology and a continuously spreading environmental awareness. If on one hand the vehicle goes in the direction of comfort, safety and reliability, on the other it has to be compliant to a set of regulations that become more and more stringent as the years go by. The global warming effect is getting worse, having catastrophic and abnormal meteorological phenomenon as a consequence. Glaciers melting, increasing sea levels, fresh water shortages, droughts, unusual storms are all issues that can be addressed to the global warming.

The cause behind this environmental problem is the green house effect. Starting way back from the industrial revolution, fossil fuel and coal have been extensively used to satisfy the energy demand. The combustion of these substances produces chemical species like CO₂ that, once the atmosphere is reached, severely interfere with the fine energetic equilibrium of the Earth. The atmospheric layers allow solar radiations to be filtered before passing through, so that the planet can be warmed up un harmfully. Eventually, the heat has to be dissipated back into the Universe, but the so-called Greenhouse Gases (*GHGs*) tend to thicken the atmospheric layers, trapping the heat inside and causing the temperature to rise. GHGs consist of a mix of gases including CO₂ which accounts for about 76% of the global human-caused emissions ^[2].

The transport sector is responsible for about 21% of total CO₂ emissions and 74.1% is coming from road transport, both for passengers and freight. This means that road transport accounts for about 15.6% of total CO₂ emissions ^[3].

GLOBAL BEV & PHEV SALES ('000s)

EV VOLUMES

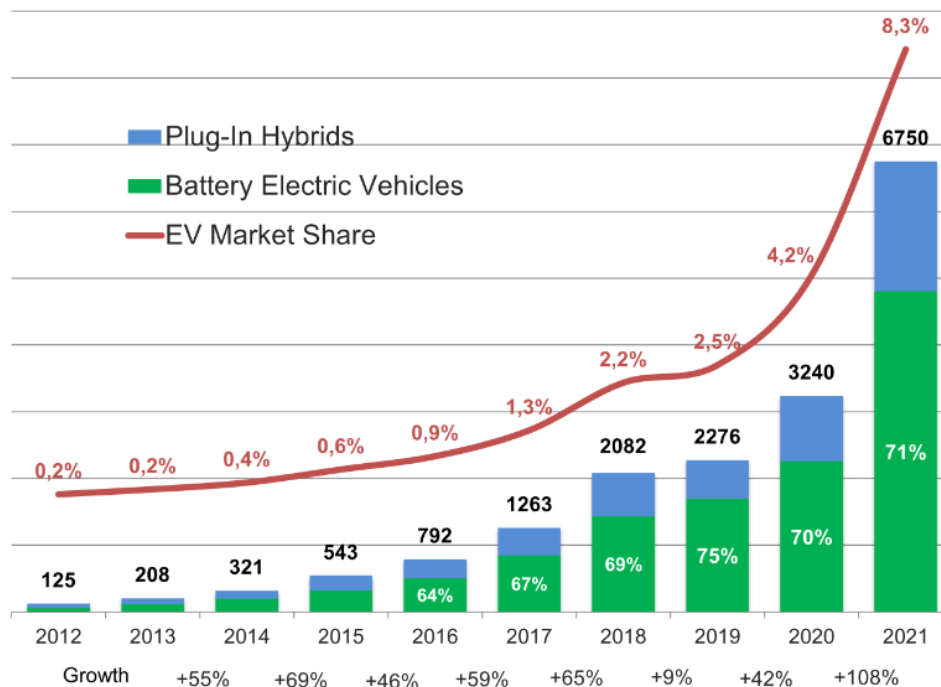


Figure 1.1 Global EV market growth ^[1]

At this point it is easy to understand why lawmakers and international entities have been setting regulations to try and lower CO₂ emission levels of road transport starting from late '90. As the targets in terms of emissions got more and more stringent automotive manufacturers have been pushed to improve conventional engines on one side, but invest in electrified powertrains on the other. In June 2021, the EU adopted a European Climate Law, establishing the aim of reaching net zero GHGs in the EU by 2050. The law sets an intermediate target of reducing GHGs by at least 55% by 2030 compared to 1990 levels ^[4]. For this reason, more and more companies nowadays are announcing pure Internal Combustion Engines (*ICE*) vehicles phase-out of their production lines by 2030, taking also into consideration the ban of ICE sales of 2035 approved in June 2022.

On the other side, the demand is also increasing rapidly. The EV market expansion is supported by local government bodies who are encouraging the population to purchase electrified powertrains, by granting discounts or incentives and by periodically forbid the circulation of specific vehicles which are not compliant with the latest emission standards.

A big portion of the EV market is represented by Battery Electric Vehicles (*BEVs*), accounting for about 71% ^[1] (*Figure 1.1*). These vehicles have zero tailpipe emissions and are considered as a potential solution to the environmental problem and to the poor air quality in urban areas. Obviously, BEVs do not come without disadvantages, regarding mostly the chemical accumulators. For reference, a conventional fuel has an energy storage capability of about 12 kWh/kg or 8.8 kWh/l, whereas a lithium battery

sets at just 0.16 kWh/kg or 0.3 kWh/l [5]; meaning that to exploit the same amount of energy a battery more than 20 times heavier than a fuel tank is needed. This obviously has an impact on a complex system such as a vehicle, which will be affected in terms of range, performance, drivability, safety and comfort. Therefore, in the current scenario, BEVs cannot compete with conventional vehicles when it comes to performance/range trade-off. That's why the researching activities are aiming at finding solutions to improve chemical accumulator's range.

However, it is not only a matter of technology of the battery itself. A crucial role is also played by the conditions the battery has to work in and by all the systems that depend on it. As a matter of fact, a chemical accumulator needs a specific range of working temperature to function properly, so it has to rely on a Thermal Management System (TMS) that preserves its life and performance in a variety of external conditions, avoiding at the same time safety issues such as battery thermal runaway and fire risks. In addition, all the auxiliaries that can be mechanically connected to an engine in a conventional vehicle, are electric in a BEV and have to adopt smart methodologies to not be sacrificing too much autonomy.

1.2 Thermal Management System

The components of a powertrain, independently from it being electrified or not, during normal operation, produce heat because of unavoidable inefficiencies. The heat rejected needs to be dissipated so that the temperatures remain in a controlled range and a proper functioning can be guaranteed, without the risk of damages of the components themselves.

In a conventional powertrain, indicatively about 30% of the fuel energy is converted into mechanical energy on the crankshaft, resulting in most of the energy being wasted in the form of heat. The heat rejected by the engine is dissipated towards the external air thanks to a relatively simple one phase coolant circuit, including a flow-generating module, a thermostat to allow fast warm-up, water jackets, a heat exchanger, a fan to increase air flow and pipings. A heater core can be paired with the main circuit to allow cabin heat up (*Figure 1.2*).

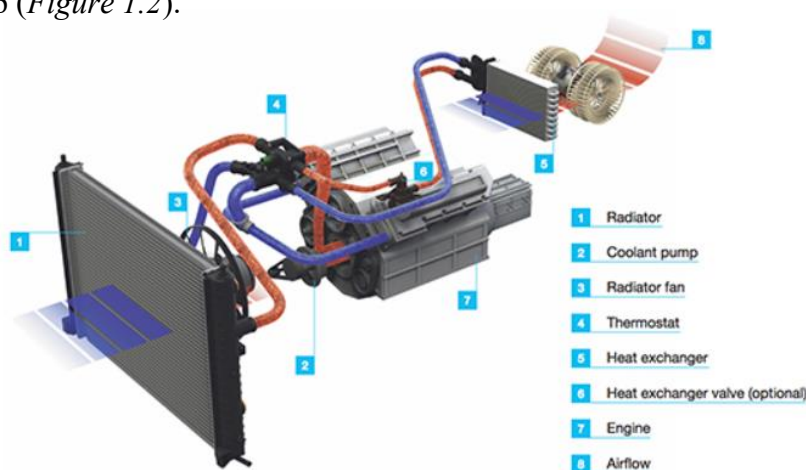


Figure 1.2 ICE Thermal Management System

As the engine gets new components (e.g. EGR circuit, turbocharger) the TMS has to adapt consequently, so that all the components can operate at their optimal temperature.

In a battery electric vehicle, the components that give the most contribution to the total heat rejection are the battery, the electric motor (or motors) and the power electronics. As *Figure 1.3* shows, each of these components needs a specific temperature window to function properly. So, even if the heat losses that the TMS has to manage is substantially lower than the conventional counterpart being EV efficiency of about 85% [6], its complexity is increased by the temperature and operating conditions requirements.

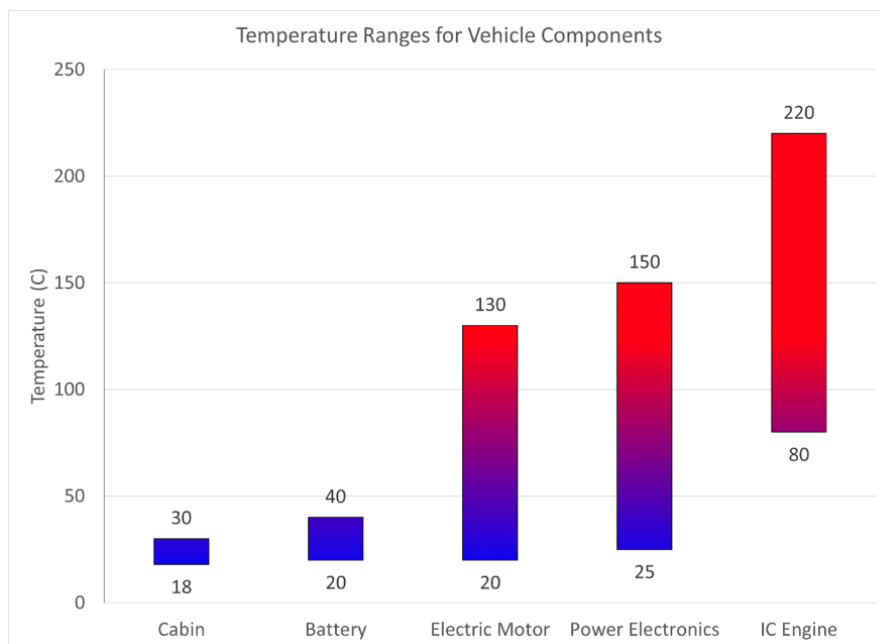


Figure 1.3 Operating temperatures for vehicle components [8]

The battery pack can be considered as the most critical component to manage from a thermal standpoint. As a matter of fact, its efficiency is extremely dependant on temperature. More specifically, researches on Lithium – ions batteries have shown that for temperatures between 15 and -10 °C, the internal resistance experiences a sensible variation, increasing up to 300%. This will in turn affect the battery capability to generate power: the more energy is dissipated internally, the less energy will be available for propulsion, thus decreasing vehicle range. The internal resistance reaches a plateau towards the high-end of the battery optimal operating range, but if temperatures get too high, the cell degradation is speeded up and the charge/discharge cycles will reduce battery life in the long term. Therefore, the accumulator has to work in a narrow range of temperature, requiring the employment of a secondary circuit in addition to the one in charge of dissipating the heat rejected by the motor and power electronics. By means of the additional circuit, the battery can be cooled down but also heated up when necessary, with or without the help of an electric heater. This is possible thanks to the pairing that it is usually made in a BEV with the Heating, Ventilation and Air Conditioning (*HVAC*) circuit. This offers several strategies to exploit, by moving around quantities of heat where it is necessary, depending on the passenger requests and

the battery conditions. For instance, if the driver requests cabin cool down and the battery pack is below the optimal temperature, heat can be taken from the cabin and given to the coolant, which eventually passes through the battery water jackets (heat pump mode). Alternatively, if the cabin requests hot air and the battery is above the optimal range, heat can be taken from the battery and dissipated into the cabin (refrigeration mode). In order to achieve these goals in an integrated system, several valves and multiple pumps are needed, as well as refined control strategies to enhance flow routing and adjust pump speeds. Consequently, the TMS becomes understandably complex, requiring a robust and reliable model to test its capabilities and to find optimized methodologies, also considering that most of the components are powered up by the battery itself, so the less energy is consumed, the longer the autonomy of the vehicle will be [7] [8].

1.3 HVAC system

For HVAC system, the whole refrigerant and ventilation group is intended, thanks to which cooling and heating of the cabin can be achieved. In order to cool down the cabin, a two-phase refrigerant fluid is employed, (R134a, R1234yf or R744 for more recent applications thanks to its lower Global Warning Potential GWP [9]) which undergoes a refrigerant thermodynamic cycle (Figure 1.4). The components involved in the circuit are:

- Compressor: generates mass flow rate, increasing fluid temperature and pressure
- Condenser: allows heat to be removed from the fluid, which becomes liquid
- Thermal or electronic expansion valve (TXV or EXV): allows fluid to expand just upstream of the evaporator (or chiller), dropping its temperature and pressure
- Evaporator: allows heat to be absorbed by the fluid, which goes back to gas state.

An overview of the architecture of the system is shown in Figure 1.5a and 1.5b.

Figure 1.5a Functional schematic of an AC circuit

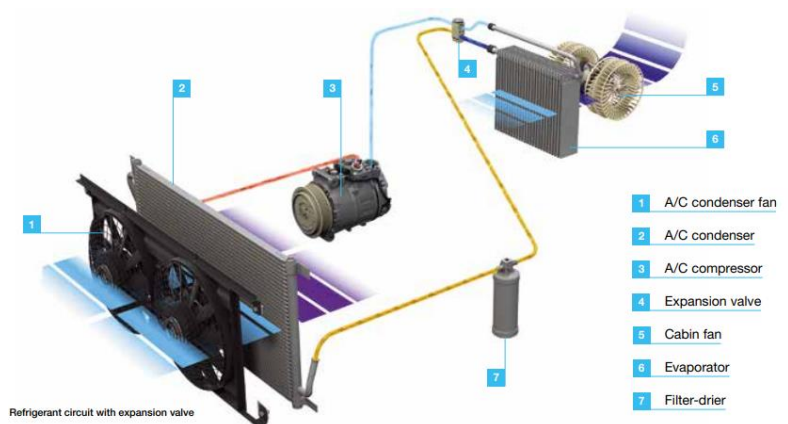
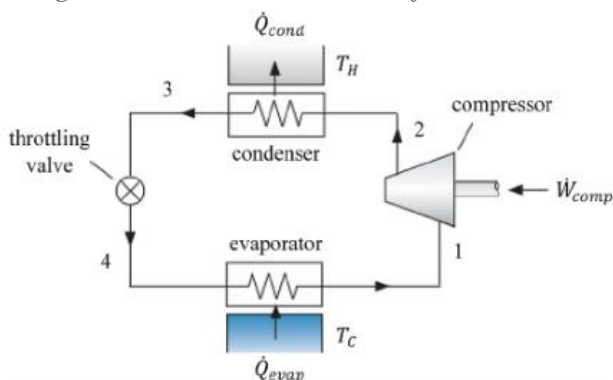


Figure 1.5b Real vehicle application schematic

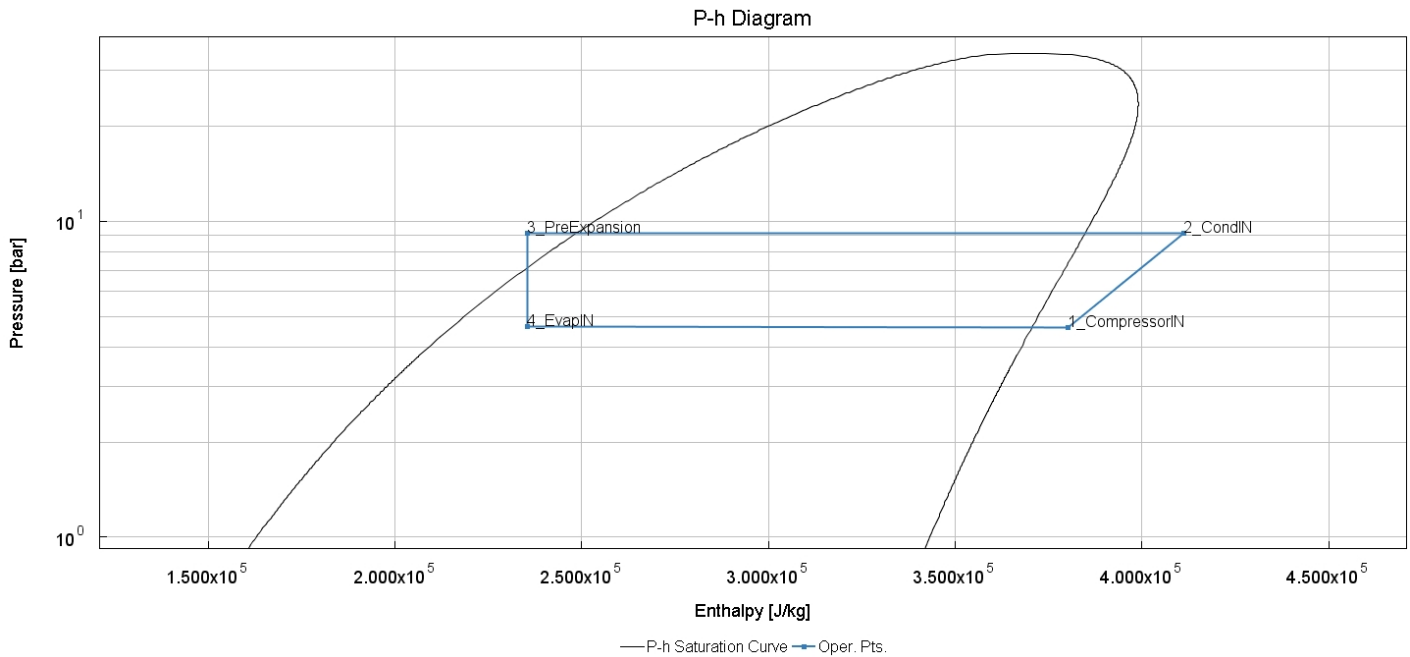


Figure 1.4 Refrigerant cycle in a p-h diagram

The p-h diagram is a useful tool to understand the thermodynamics behind the cycle. The black bell-shaped curve is called saturation curve, and it determines the phase of the refrigerant: on the right of the curve, the fluid is in gaseous phase, on the left the fluid is in liquid phase and inside of the curve the fluid is composed by a mix of the two phases; the physical quantity used to establish the phase composition inside the curve is the *vapor quality*, evaluated as the vapor mass over the total mass of fluid.

The cycle has to be read anti-clockwise, starting from the compressor. In *state 1* the fluid has to be all gaseous to preserve the component integrity. As a matter of fact, a certain amount of superheat is targeted at the compressor inlet by controlling the opening area of the TXV. After the evaporation is complete, the fluid keeps increasing its temperature of a specific ΔT before entering the compressor. The target depends on the type of refrigerant used, 5-15K for R134a, 10-25K for R1234yf or 25K for R744. Graphically, the superheat can be visualized as the horizontal segment between the saturation curve and *state 1*, indicating that the fluid is moving away from the saturation line increasing its temperature and superheat level. At this point the refrigerant gets compressed and reaches *state 2*: the energy that the compressor gives, causes pressure and temperature to rise; final values depend again on the type of fluid used, but also on operative conditions, TXV counterpressure etc. In the condenser the gas dissipates heat into the external environment, changing its phase into liquid and dropping its temperature of a specific ΔT after the condensation is complete. This is called subcooling, it's the same principle of the superheat but mirrored on the condenser side and can be visualized as the horizontal segment between the saturation curve and *state 3*. Between *state 3-4* the fluid passes through a regulated orifice and gets expanded; pressure and temperature drop consequently. Segment 3-4 represent the evaporation phase, in which the refrigerant absorbs back part of the heat it had released during condensation and changes phase back to gas.

Figure 1.5b is useful to understand how a real vehicle application is implemented. The compressor can be mechanically connected to the engine via belt/chain connection or can be electric for better control purposes. The condenser is placed in the underhood radiator pack, together with the other vehicle radiators; air flow can be improved by the fan. The evaporator is placed closer to the cabin and it is paired with a blower so that warm air can be cooled down and enter the cockpit through the vents.

For electrified powertrains, the air conditioning system is paired with the main cooling system, opening up the methodologies to choose to several combinations of thermal management requests by different components. Usually, the pairing is done by introducing a new component, the chiller. It is substantially another heat exchanger, commonly of the plate type, that allows energy to be exchanged between the refrigerant circuit and the cooling battery circuit. Depending on the capabilities of the whole system, from the HVAC circuit point of view, it can function as a condenser, so that the refrigerant releases heat to the coolant (heat pump mode), or it can work as an evaporator, so that the refrigerant absorbs heat from the coolant (cooling mode).

In order to be able to switch the operating principle of the chiller, as well as manage driver AC requests and keep under control all the temperatures, several solenoid valves (*EVs*) are usually employed in the HVAC system and in the cooling system. Their main purpose is to divert the flow of refrigerant or coolant towards a component or another, following a logic that keeps into account different scenarios, case by case.

Although the general functioning of a BEV TMS has been explained, the methodologies, the components, the type of solenoid valves and the circuits themselves depend on the specific vehicle application. Therefore, in the next section, some real-world examples are given, selecting the solutions that share characteristics with the model that has been built and that will be presented in *Chapter 3*.

1.4 BEV Thermal Management System solutions

1.4.1 Fiat 500e TMS

In *Figure 1.6* the schematic of the Fiat 500e TMS is shown. It consists of three loops, one for the power electronics, electric motor and on-board charger (*green loop 3*), one for the HVAC module (*blue loop 2*) and one for the battery (*yellow loop 1*). *Loop 1* and *2* are coupled together by a chiller heat exchanger, which works in parallel with the cabin evaporator. Depending on the case, the two XV's can be controlled so that either the cabin, the battery or both can get cooled down. The cabin heat up is managed by a 5 kW electric heater, which warms the cold air passing through the evaporator up to the target temperature. Also the battery warm up is managed by an electric heater (7 kW); in the shown configuration, no heat pump mode is available. As a matter of fact, the loops are relatively simple, just two three-way solenoid valves are used in *Loop 1*, managing the cold/hot flow coming from the chiller, main radiator or heater ^[10].

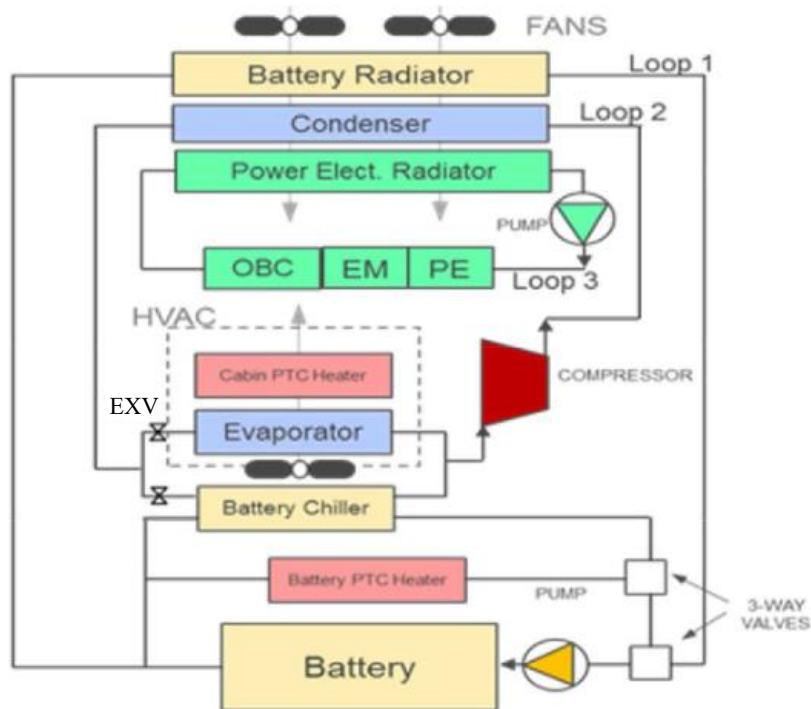


Figure 1.6 Fiat 500e BEV Thermal Management System ^[10]

1.4.2 Tesla Model S (2013) TMS

In *Figure 1.7* the schematic of the Tesla Model S TMS is shown. Differently from the Fiat 500e circuit, Tesla chose to use just two loops, the HVAC one (in *blue*) and the main coolant one (in *black*), where the battery pack and the propulsion unit are linked in series. The two circuits are again coupled by the chiller, that can be used to further cool down the battery. The heat up of both battery and cabin is managed by an electric

heater; no heat pump is employed in the configuration depicted in *Figure 1.7*. The vehicle has received that upgrade starting from the 2021 version of the model. In this case, the flow of the main circuit is diverted by 2 3-way valves and a 4-way valve. The 4-way EV is used to make a single circuit if the battery temperature is below the limits (depicted configuration) or split it in two if the desired range is reached, relying on the chiller for cooling. On the other hand, the 3-way valves are used to bypass the radiator or the chiller in case warm up is needed ^[11].

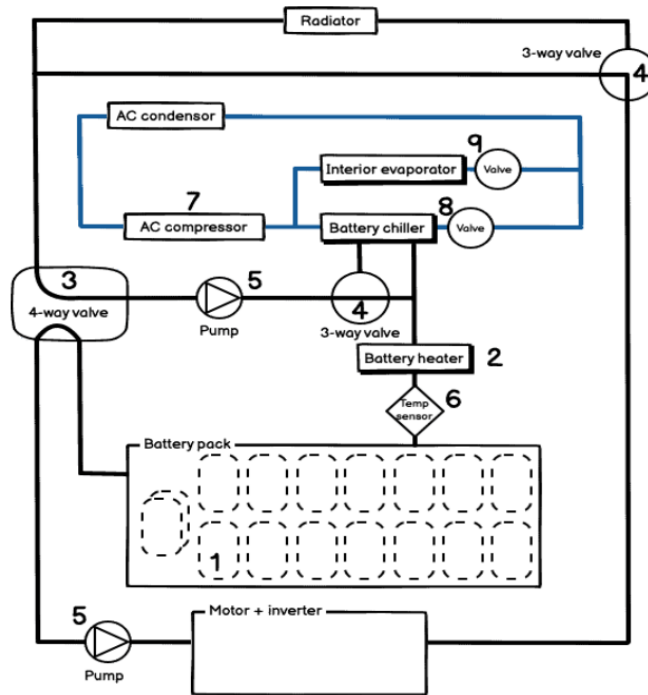


Figure 1.7 Tesla Model S Thermal Management System ^[11]

1.4.3 Tesla Model Y (2019) / Model S and X (2021) TMS

Starting from 2021, the refreshed versions of Model X and Model S received the improved Thermal Management System that was firstly introduced in the Model Y ^[12]. The new TMS introduced a lot of complexities in the circuit, but it also improved the overall efficiency of the system, that, in turn, benefits the range of the vehicle. A schematic of the circuit can be seen in *Figure 1.8*: the coolant flow is highlighted in *blue*, the refrigerant flow is highlighted in *red*. It can be noticed that the main components of the circuits are indicatively the same of the previous configuration; the real game-changer is the 8-way valve. It gives to the system incredible flexibility and the capability to adapt to several operating conditions and thermal requests: the TMS patent ^[13] states that it is possible to have 12 different heating modes and 3 cooling modes. The chiller is always used as an evaporator, but the introduction of the Liquid Cooled Condenser (*LCC*) and the cabin condenser, allow the use of the heat pump mode, saving the energy that would have been used by an electric heater, improving in turn, the range of the vehicle. A 12V heater is still present, but it is used as an auxiliary component rather than the main solution to heat up the cabin. Depending on the case, the four 3-way valves in the refrigerant circuit divert the flow deciding which heat

exchanger has to release heat to the refrigerant fluid (LCC or Cabin Condenser) and which one has to absorb heat from it (Cabin Evaporator or Chiller). On the coolant circuit, the 8-way valve works synchronously to connect different branches and decide which component has to be warmed up, and which one has to be cooled down. In addition, the 3-way valves installed in the coolant circuit are used to bypass parts of it. Therefore, using different combinations of the valves' position, heat can be extracted from various sources and given where it is necessary. As a matter of fact, battery can be warmed up by connecting its water jackets with the LCC or can be cooled down by connecting it to the radiator or chiller or both. On the other hand, the cabin can be warmed up by the battery heat extracted by the chiller or can be cooled down releasing heat into the environment or to the battery coolant circuit [14].

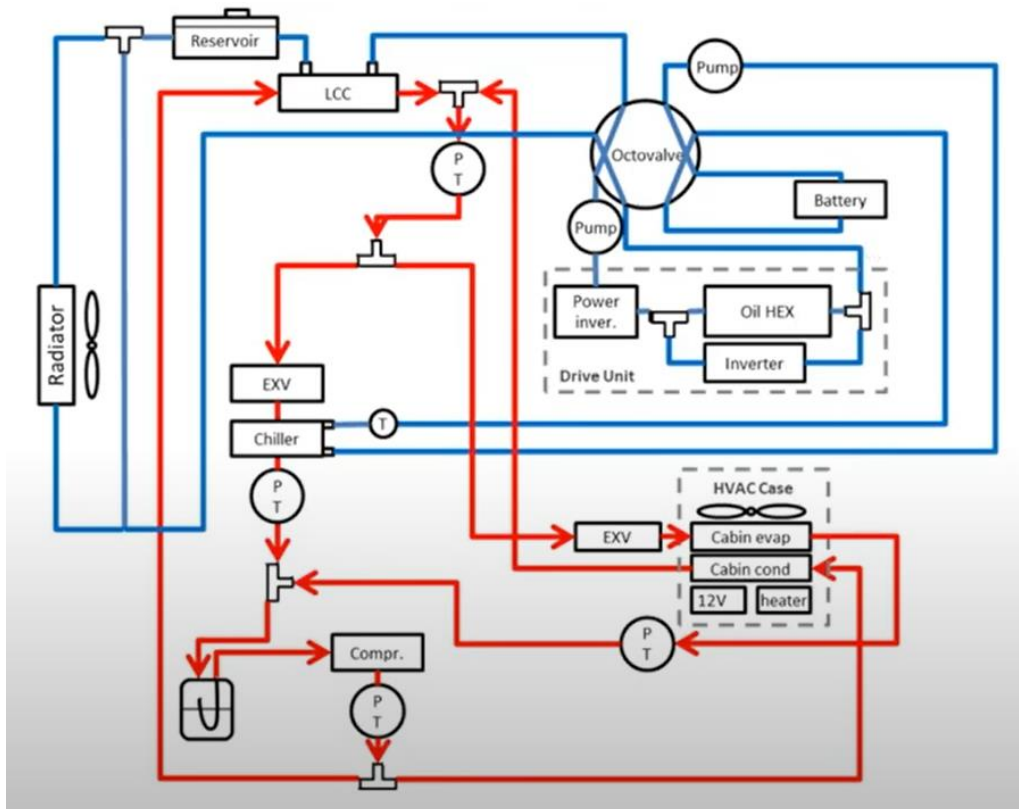


Figure 1.8 Tesla Model Y Thermal Management System [14]

The solutions that have been presented in the last section have different degrees of complexity. The model that has been built and that will be presented in *Chapter 3*, is inspired by the shown configurations but has been chosen to have an intermediate level of complexity: it does not have an 8-way valve, but it does offer the possibility to use heat pump mode, together with normal refrigeration mode.

Chapter 2

1D Software – GT SUITE

The model that will be presented in *Chapter 3*, has been built by means of GT-SUITE. It is a CAE (*Computer Aided Engineering*) software developed by Gamma Technologies LLC, a US company leader in offering comprehensive and integrated simulation tools, intended for a wide range of application, from automotive to aerospace, from marine to rail.

The software offers a 1D modelling environment, using a 1D discretization method to describe components with a dimension significantly greater than the other two, such as pipes. For this reason, GT-SUITE is particularly suited to model and simulate thermal management systems, especially when integrated with propulsion models and vehicle models.

The 3D modelling option is also available by means of an extension to the main software called COOL3D, useful tool to recreate in a 3D environment the underhood configuration of heat exchangers, the presence of obstacles obstructing the air flow rate, the actual shape of air volumes and so on. However, it is not a proper 3D simulation (usually it is referred as quasi-3D), as the model is automatically converted and discretized into 1D environment to be runnable. For the purpose of the project, COOL3D will not be used and a 1D solution is chosen to model the underhood components. Mono-dimensional simulation show a good trade-off between accuracy of the results and computational time. Usually, a 3D-CFD simulation does offer a more detailed outcome, but the significantly higher requested computational power and longer calculation times limit its use to specific applications, for instance to in-cylinder charge motion analysis. For this reason, three-dimensional simulation cannot be employed for an integrated model as the one of this project analysis.

GT-SUITE library offers a wide variety of templates to use, regarding flow, thermal, mechanical, electromagnetic and controls modelling. Thanks to this possibility, the controls logic on the HVAC circuit and on the compressor speed can be developed and the best methodology can be selected in order to achieve specific targets in the most convenient way possible.

2.1 Flow solution method

Since GT-SUITE is a 1D simulation software, flow systems are discretized in one direction, according to the discretization length that has been set and to the component in exam. For instance, a pipe will be divided into sub volumes, on the other hand a flow split component that is usually used to model volumes, will always be considered as a single element. The discretized elements are interfaced to each other by boundaries, at which vector quantities such as mass flux and velocity are calculated. Scalar quantities such as pressure, temperature, density, enthalpy and mass concentration are assumed uniform over the discretized volumes and are evaluated at their centroid (*Figure 2.1*).

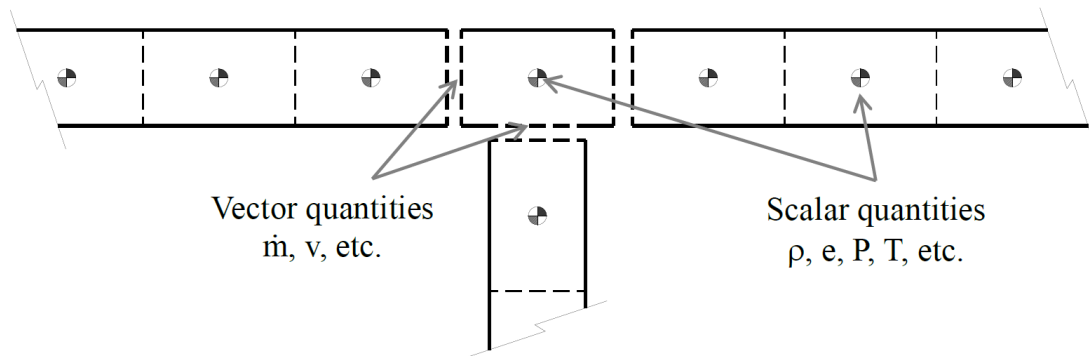


Figure 2.1 Components discretization

The calculation method evaluates those quantities by numerically solving the Navier-Stokes equations (*equations 2.2 to 2.5*), including mass and energy conservation to compute the thermodynamic state of each volume and the momentum conservation to compute the vector quantities at the boundaries. These equations are solved along one direction, therefore all the calculated quantities are averaged along the direction of the flow.

The integration method GT-SUITE offers, can be chosen between an explicit solver and an implicit solver.

The explicit solver's main variables are mass flow rate, density and internal energy and they are evaluated starting from the values of the neighbouring discretized volumes at the previous timestep. As a consequence, the primary variables derivative is found, and all the values at the new timestep can be evaluated by integration over the timestep. Therefore, an iterative procedure is not employed and the timestep has to be chosen small enough (10^{-4} to 10^{-6} seconds) to achieve Courant stability condition:

$$\frac{\Delta t}{\Delta x} (|u| + c) < 0.8 \quad (2.1)$$

where Δt is the timestep, Δx is the discretization length, u is the fluid velocity and c is the speed of sound.

Since the explicit method requires small timesteps, this solver is mostly suitable for simulations where unsteady flow, pressure pulsations, high frequency wave dynamics are of interest. However, that is not the case of this thesis, in fact cooling systems have a time scale that is relatively long, therefore an implicit solver is advised to be used.

The implicit solver's main variables are mass flow rate, pressure and total enthalpy, calculated by solving a non-linear system to find the values of all sub-volumes at the current time step simultaneously. Since this is an iterative procedure, longer CPU computational time is requested, but the timestep that the solver can take is much larger, in the order of 0.01 to 0.1 seconds, and this will ultimately outweigh the CPU cost. The greater timestep of the implicit method makes the relative solver mostly suitable for simulations where pressure pulses or wave dynamics accurate predictions are not of interest. In a generic cooling system, the implicit solver is really efficient, therefore this is the one chosen for the project. In the run setup of GT-SUITE, four different circuits will be identified, and an implicit solver will be assigned to each of them. The four circuits are: cooling circuit, refrigerant circuit, cabin air circuit and underhood air circuit [15].

$$\text{Continuity: } \frac{dm}{dt} = \sum_{\text{boundaries}} \dot{m} \quad (2.2)$$

$$\text{Energy: } \frac{d(me)}{dt} = -\rho \frac{dV}{dt} + \sum_{\text{boundaries}} (\dot{m}H) - hA_s(T_{fluid} - T_{wall}) \quad \text{(explicit solver)} \quad (2.3)$$

$$\text{Enthalpy: } \frac{d(\rho HV)}{dt} = \sum_{\text{boundaries}} (\dot{m}H) + V \frac{dp}{dt} - hA_s(T_{fluid} - T_{wall}) \quad \text{(implicit solver)} \quad (2.4)$$

$$\text{Momentum: } \frac{d\dot{m}}{dt} = \frac{dpA + \sum_{\text{boundaries}} (\dot{m}u) - 4C_f \frac{\rho u |u|}{2} \frac{dxA}{D} - K_p \left(\frac{1}{2} \rho u |u|\right) A}{dx} \quad (2.5)$$

\dot{m}	boundary mass flux into volume, $\dot{m} = \rho Au$
m	mass of the volume
V	volume
p	pressure
ρ	density
A	cross-sectional flow area
A_s	heat transfer surface area
e	total specific internal energy (internal energy plus kinetic energy per unit mass)
H	total specific enthalpy, $H = e + \frac{p}{\rho}$
h	heat transfer coefficient
T_{fluid}	fluid temperature
T_{wall}	wall temperature
u	velocity at the boundary
C_f	Fanning friction factor
K_p	pressure loss coefficient (commonly due to bend, taper or restriction)
D	equivalent diameter
dx	length of mass element in the flow direction (discretization length)
dp	pressure differential acting across dx

Figure 2.2 Navier-Stokes equations

2.2 Thermal management system modelling

As shown in *Section 1.4*, a thermal management system includes several sub-systems that interact with each other through heat exchangers. These systems consist in coolant, HVAC and air circuits that are made up by different components, such as radiators, fans, pumps, valves and pipes. Consequently, a comprehensive CAE tool is needed to run TMS simulations, and GT-SUITE is specifically designed to manage this wide variety of sub-systems.

In the mono-dimensional environment offered by GT-SUITE, several parallel fluid circuits can be built simultaneously, and the task is simplified by the object-based approach the code is designed with. The versatile graphical interface, GT-ISE (*Integrated Simulation Environment*), allows the user to select desired templates from the library, create sets of objects with different characteristics and deriving from them the actual components that can be dragged and dropped into the map, with the possibility of trying out different layouts. Components from the same object share the main characteristics, but each inserted data can also be override in the specific component. In addition, by arranging the library with different templates, GT-ISE also minimizes the amount of input data required from the user, leaving just the fundamental geometrical elements to be defined. For example, if the user wants to model a heat exchanger, the library offers a lot of templates he can choose from according to the needs, including plate heat exchangers, tube-fin heat exchanger, shell-tube heat exchangers. In this way, the user can already select the type of exchanger he needs, making easier his task to build the model.

Specifically speaking, a heat exchange between two fluid circuits can be modelled using the main and secondary pair. They are two distinct elements that have to be inserted into the two circuits the heat is exchanged between. GT-SUITE discretizes the geometry to create a model of the heat exchanger able not only to predict the heat transfer performance within its input data range, but also in conditions that are outside the input map, that is usually a reference map provided by the supplier and built during component free-flux testing. The convective heat transfer calculation in each sub volume from the fluid to wall, is based on heat transfer coefficients, defined by the Nusselt number correlation in the form:

$$Nu = C Re^m Pr^{1/3} \quad (2.6)$$

where Re is the Reynolds number, Pr is the Prandtl Number, C and m are constants depending on the geometry and flow conditions and are evaluated starting from steady-state experimental data.

Cooling circuit pumps can be modelled in a similar way of the compressor used in the HVAC circuit. A performance map has to be defined, inserting the data of pressure rise and volumetric flow rate in function of pump speed. In addition, the pump type and inertia can be specified; also data about milling and reverse leakage when the pump is

off can be included. The pump (or the compressor) can be modelled as mechanical, so that the speed can be directly imposed by a parameter or by an external object, or as electrical, so that the input signal can be imposed. The last option gives better flexibility if a certain control strategy has to be applied or if the pump is in a full electric application such as a BEV ^[16].

Also fans (or blowers, for the cabin air circuit) can be modelled as mechanical or electrical. They require geometrical properties as input data as well as a reference map in which pressure rise and mass flow rate are shown in function of the speed. Similarly to pumps, milling data can be inserted as well.

As far as HVAC systems are concerned, their modelling can be performed by using components such as pumps/compressors and heat exchangers that have been already described. In addition, a two-phase fluid circuit requires also expansion devices, in order to make the flow expand to a low pressure state and to allow the phase shift. These devices can be modelled in GT-SUITE by thermal or electronic expansion valves. The first kind needs a 4-quadrant diagram, correlating valve lifts, refrigerant mass flow rate, evaporator outlet pressure and temperature data. The latter kind, on the other hand, requires a certain control strategy that regulates the valve flow area. This will be the expansion device used in the model that has been built for this thesis.

The cabin circuit is a fundamental part of the air conditioning model, as its feedback affects the performance of the whole system. The cabin can be modelled with different levels of accuracy, from lumped volume model to fully discretized COOL3D based model to interface with CFD. For this project, the lowest computationally demanding model has been selected, so all the air is represented by a single volume. GT-ISE offers different templates according to the size of the vehicle, each one with several data already pre-filled. Some of the inputs still to be defined are: ambient temperature, vehicle speed, solar flux, soak state.

The piping network has a considerable impact on the performance of the system too. In GT-SUITE, it can be modelled by different types of pipes and flowsplit templates, so that the actual shapes can be matched, obviously within the limitations of a 1D environment. In this thesis, just straight pipes have been used, giving the geometrical characteristics as an input. All the network has been chosen to be adiabatic, except for the flowsplits component used to model the water jackets of the several heat sources in the coolant circuit ^[17].

Chapter 3

Thermal Management System Model

The entire Thermal Management System is shown in *Figure 3.1*. It includes an underhood circuit, a coolant circuit, an HVAC circuit and a cabin circuit, all coupled together by heat exchangers. The model has been built taking into account different BEV solutions and although it does not refer to a specific application, all the inserted inputs, maps and measures have been thought to be as close to reality as possible, since they are the results of data coming from literature and open GT-SUITE libraries and examples. For what the layouts are concerned, the coolant, the underhood and the cabin circuits have been chosen on the basis of a generic BEV TMS, the HVAC circuit, on the other hand, has been adapted to be able to cover all the possible combinations of battery and cabin heating/cooling and more or less severe environmental conditions, introducing both cooling and heat pump mode. In the following sections, the different circuits will be discussed in detail.

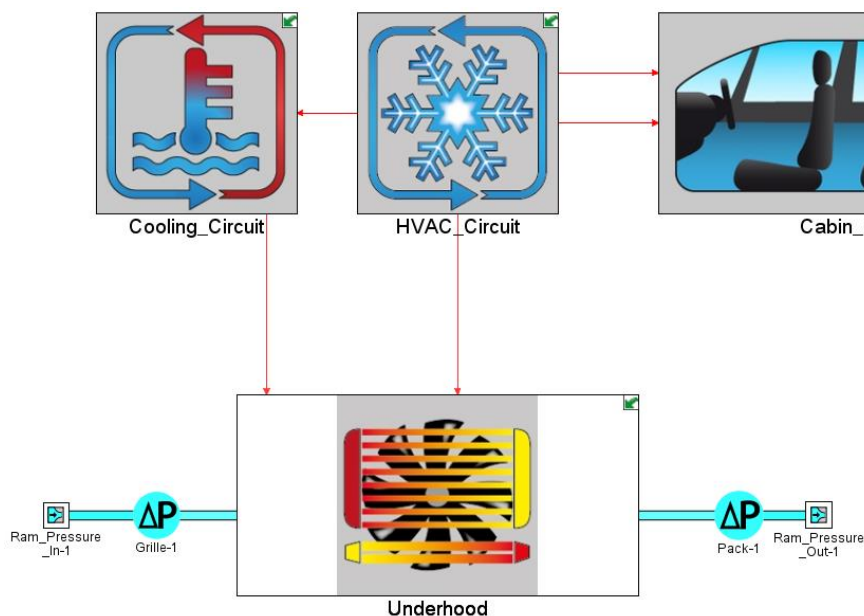


Figure 3.1 Thermal Management System Model

3.1 Cooling Circuit

Figure 3.2 shows the layout of the cooling circuit. The reference fluid is *egl-5050* (50% ethylene glycole by volume).

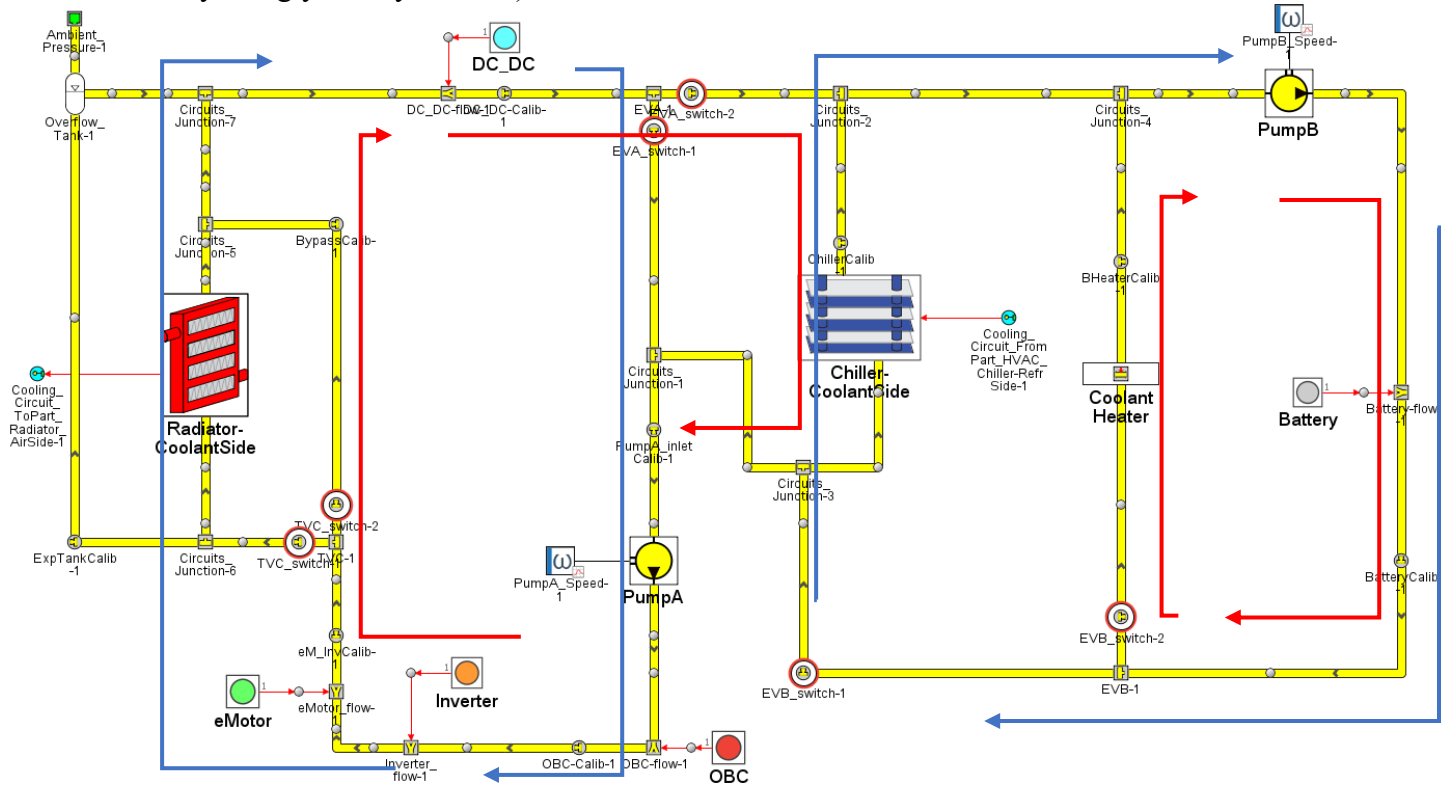


Figure 3.2 Cooling circuit

The circuit appears relatively complex, as it is composed of different components. In addition, 2 3-way valves and 1 continuous valve in charge of diverting the flow. The components rejecting heat are the DC/DC converter, the On Board Charger (OBC), the inverter, the electric motor, which are connected in series and the battery, which is cooled by another branch. As the purpose of the study was not focused on this circuit and no further data were available (such as a CAD file), those elements have been modelled as simple thermal masses which reject heat to the relative FlowSplit, used to model the internal water jackets. In the Table 3.1 the used that are shown.

COMPONENT	MATERIAL	HEAT REJECTED [KW]
DC/DC	Silicium	0.67
OBC	Aluminium	0
INVERTER	Aluminium	2
E-MOTOR	Custom*	9
BATTERY	Aluminum	sweep (Sect 3.5)

Table 3.1 Data used to model heat-rejecting components

*The thermal characteristics of the e-Motor has been chosen to take into account the presence of different materials and it is reported in *Figure 3.3*.

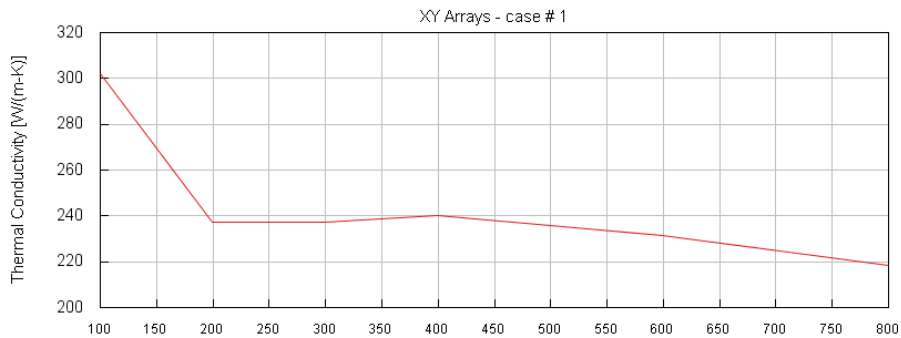


Figure 3.3 eMotor Thermal characteristics

The inserted heat rejection quantities are purely indicative, as the focus of the study was on the HVAC system and its interaction with the cooling circuit. For this reason, the battery has been tested separately, results will be discussed in *Section 3.5*.

The quantity of heat introduced into the circuit is dissipated by the radiator and the chiller. The main coolant-side radiator is coupled with its secondary air-side template in the underhood circuit, and its dimensions have been chosen to be 550x350x21mm. It has a thin tube, horizontal, single pass configuration, with 64 tubes in the first row. Depending on the external conditions and the temperature of the powertrain components, the main radiator can be bypassed by a continuous valve (*TVC* on the map, highlighted in red) in order to allow fast warm-up. The percentage of bypassing flow can be decided adjusting the passage area or the discharge coefficient. In addition, a 1.8L overflow tank has been added to account for thermal fluid expansion.

On the other hand, the chiller is modelled with a secondary template, coupled with its main counter part in the HVAC circuit. It is of the plate type (70x45mm), with a 3-pass configuration for a total of 10 channels. It is connected with the battery cooling circuit and according to the methodology used in the HVAC system, it can be employed to warm up or cool down. Also, an electric coolant heater is added, so that it can be turned on either if the heat pump doesn't produce enough heat, if the warming process is quick and not that intensive or if the heat pump mode cannot be activated.

The flow is generated by two pumps (*PumpA* and *PumpB* in the map) and managed by two 3-way valves. The pumps are of centrifugal type and are modelled so that a constant speed value could be passed. The working map can be seen in *Figure 3.4*, built considering similar applications. Same considerations have been drawn for the pipings, modelled with adiabatic straight pipe templates with a diameter of 15mm and a length depending on the position of the components they connect to. For instance, the pipes connecting the e-Motor to the radiator have a length of 2000mm, simulating the connection with a machine mounted on the rear axle.

The 3-way valves (*EVA* and *EVB*) are in charge of switching between two circuit configurations. They are modelled with *FlowSplit* templates to simulate the volume of the valves themselves, plus 2 custom connections at the outlets (highlighted in red on

the map) with a parameterized forward and reverse coefficient. Looking at *Figure 3.2*, the *blue* configuration splits the cooling circuit in two: one is managed by the radiator, dissipating the heat coming from DC/DC, inverter, motor and OBC, the other is managed by the chiller, in charge of cooling down (or heat up) the battery. On the other hand, the *red* configuration allows the battery to be warmed up by the electric heater, letting the radiator and the chiller manage together the heat rejected by the other components. In addition, depending on the operating conditions, the radiator can be partially or totally bypassed and the chiller can warm up the coolant if the heat pump mode is active in the HVAC circuit.

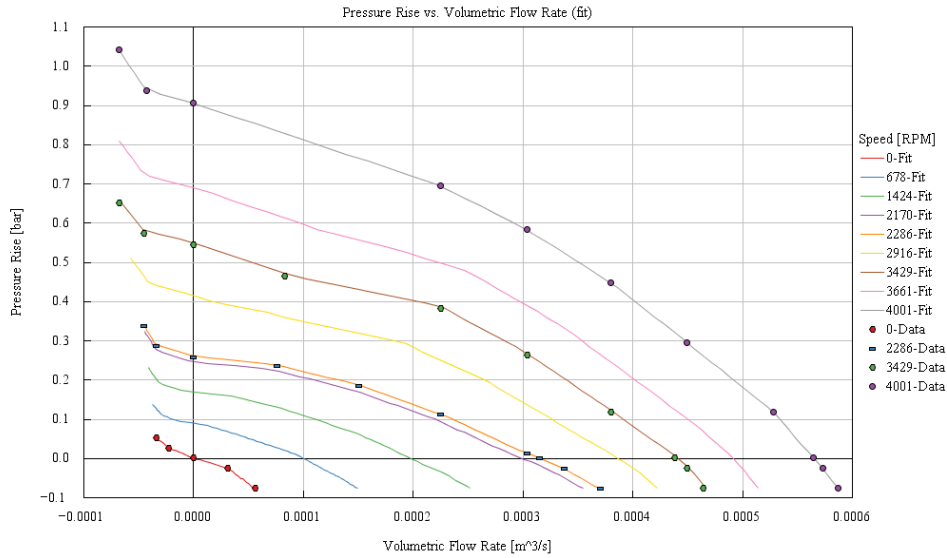


Figure 3.4 Pumps operating map

To conclude the discussion, several custom orifices can be noticed in the circuit (e.g downstream of the heater, battery, chiller and so on). Their diameters have been calibrated by means of iteration procedures in order to reach the realistic flow rate targets of 12 L/min in PumpA circuit and 10 L/min in PumpB circuit at maximum pump rpms, without exceeding a pressure level of 2 bar. In practice, by imposing smaller diameters than the pipe ones in localized sections of the circuit, flow resistance is introduced. This causes the pumps to work at higher pressures, producing less flow rate as a consequence. The calibration diameters have therefore been chosen to achieve realistic values of pressure and flow rate at the same time.

In the following sections and in the results that will be presented, the configuration used in the cooling circuit is the *RED* one, as the focus of the project has been on testing and calibrating controls in the HVAC circuit, monitoring their effects on the battery.

3.2 Underhood circuit

For what the underhood model is concerned, a simple mono dimensional circuit has been used (*Figure 3.5a*), built with GT-SUITE map tools.

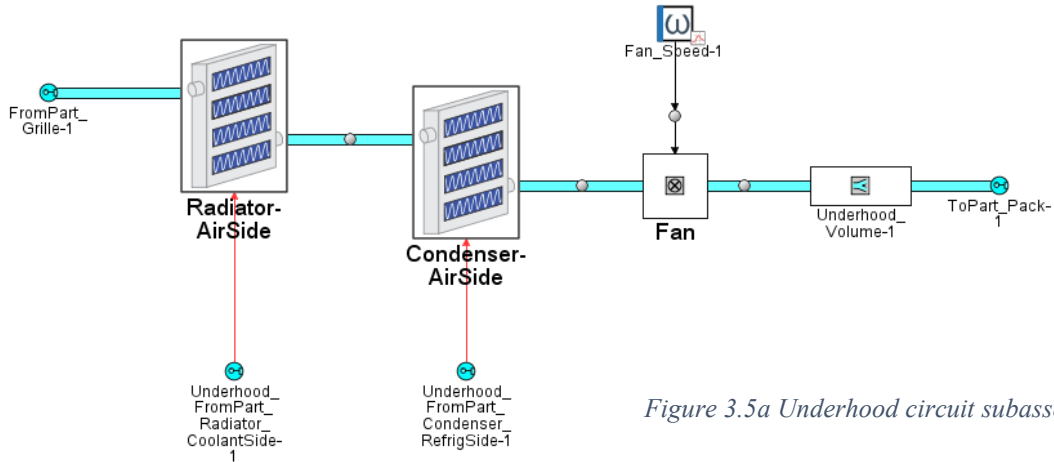


Figure 3.5a Underhood circuit subassembly

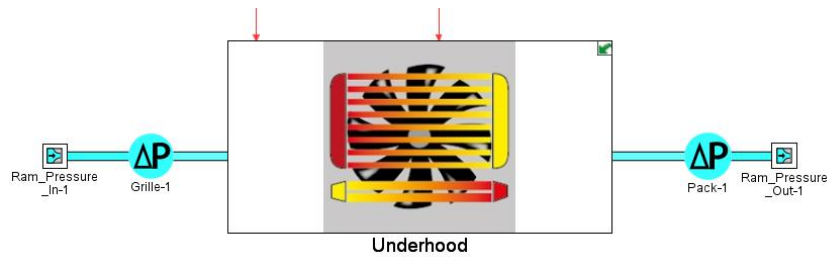


Figure 3.5b Underhood subassembly external connection

Apart from the subassembly itself, two localized pressure loss connections have been added to model pressure drops caused by the grille and the radiator pack. In addition, external boundary conditions had to be imposed and thanks to the RamPressure template the quantity of air flow can be linked to the vehicle velocity, given to the TMS as a parameter since no vehicle model has been provided.

Looking at the proper circuit in *Figure 3.5a*, the underhood is modelled with a simple volume of 80L, in which a fan blows the air that absorbs heat from the coolant in the radiator and from the refrigerant in the condenser. In the shown subassembly, the secondary air-side templates of the two heat exchangers can be seen.

The fan has been chosen to have a blade diameter of 400mm, a hub diameter of 125mm and a depth of 25mm. *Figure 3.6* shows its working map.

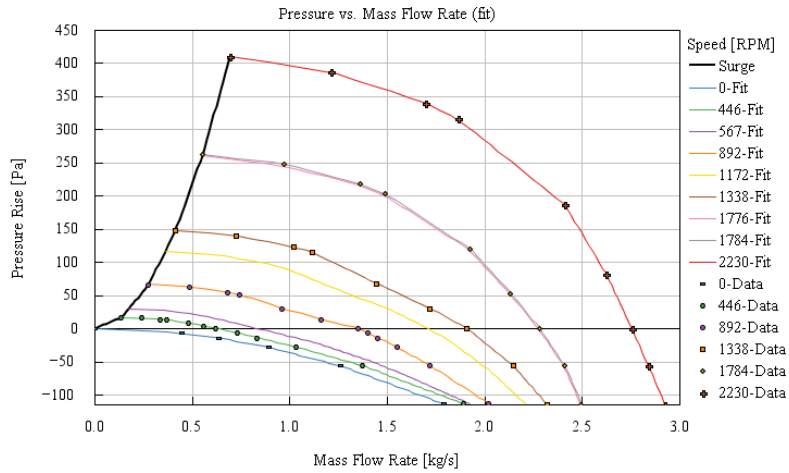


Figure 3.6 Fan working map

3.3 HVAC circuit

In Figure 3.7, the layout of the HVAC circuit can be explored. The discussion of this circuit will be divided in three sections, in order to better clarify the developed control strategies.

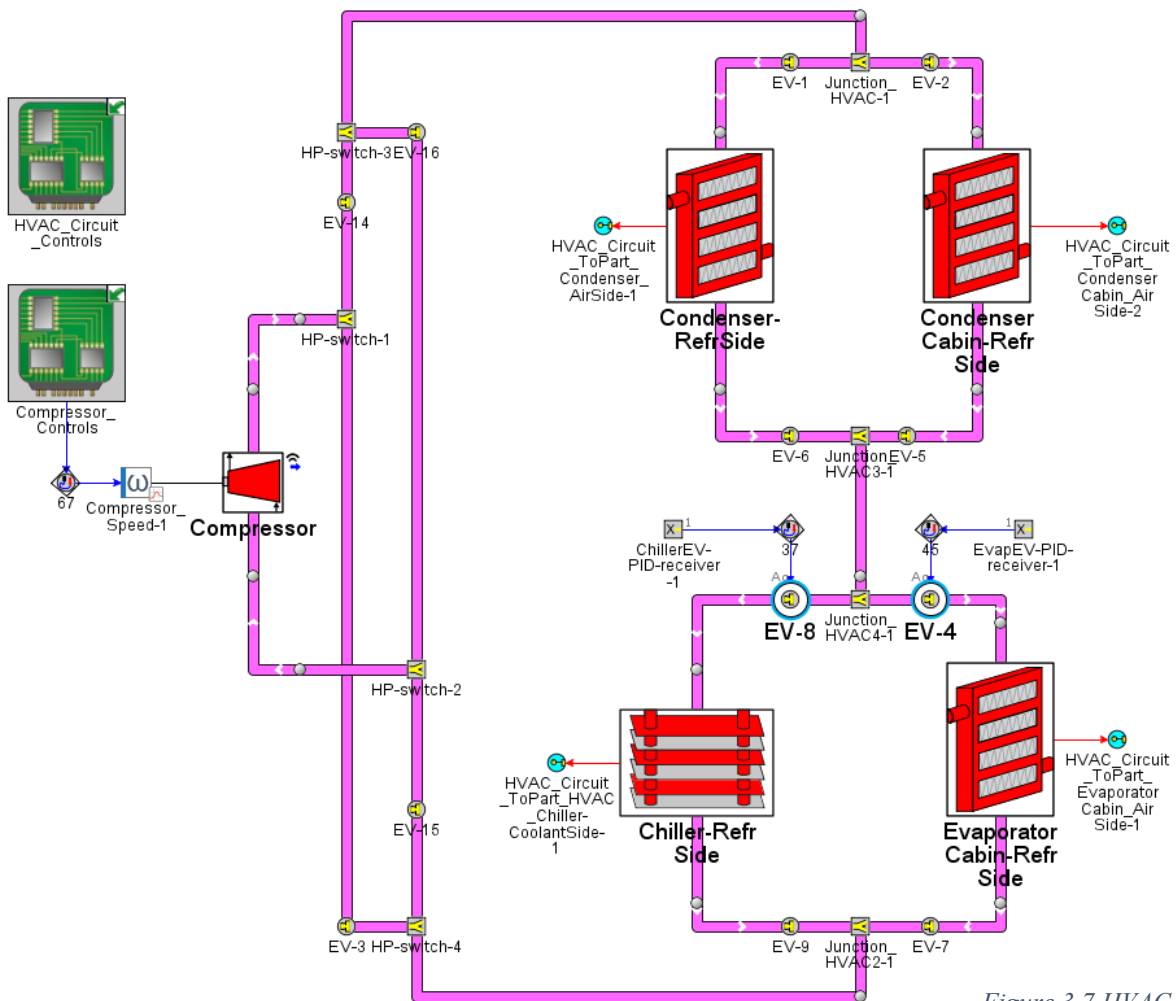


Figure 3.7 HVAC circuit

3.3.1 Model and layout description

The refrigerant fluid for this circuit is the R1234yf and a total charge of 0.85Kg has been used to test the system. The main components are the ones of a common HVAC circuit, as described in *Section 1.3*. The compressor works according to a map taken from similar applications found in the GT open library (*Figure 3.8*), and its speed is controlled by an additional module. The two condensers are the main refrigerant-side templates coupled with the underhood condenser and the cabin condenser, respectively. They are both thin tube heat exchangers, but the underhood one has an horizontal configuration (550x350x20mm) with 2 passes and a total of 50 tubes in the only row, the cabin one has a vertical configuration (250x300x25mm) with 3 passes and a total of 22 tubes in the only row. So, it is reasonable to say that different heat exchanges are expected.

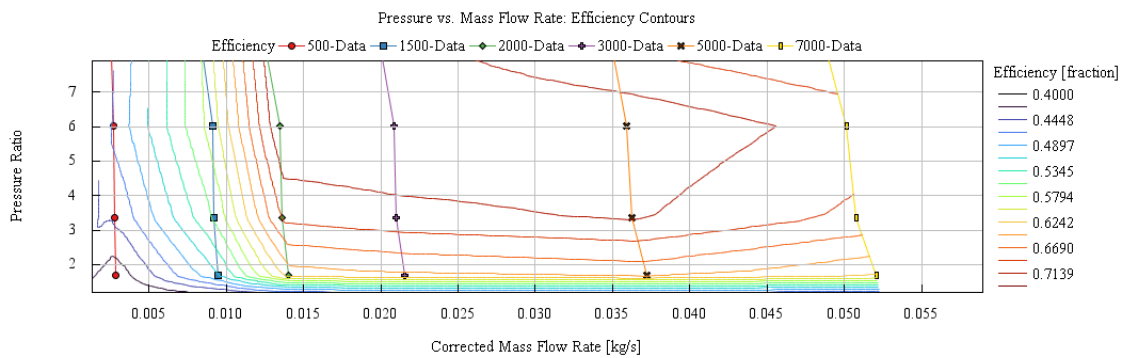


Figure 3.8 AC Compressor working map

The two condensers are used alternatively depending on the passengers AC requests. If the passengers activate cabin heating, the underhood condenser is not used, so that the heat coming from the battery and dissipated by the chiller can be re-used and not wasted in the environment. On the contrary, if the AC request is off or the conditions are such that it is more convenient to use the electric heater, the underhood condenser can receive all the flow. The refrigerant flow diversion is managed by *EV1* and *EV2*, two simple open/closed solenoid valves. Two additional similar connections (*EV5* and *EV6* or *EV9* and *EV7*) are employed also at the outlet of the heat exchangers so that the one that is not active cannot alter the fluid state in any way. These connections are not real valves, as they represent a workaround needed to avoid numerical problems. For what the evaporators are concerned, the chiller in the map is the main refrigerant-side template coupled with the coolant circuit and it has been already described in *Section 3.1*. The other evaporator is coupled with the cabin circuit and therefore it is used to cool down the cabin when the AC request is on. The specs of the cabin side evaporator include a thin tube exchanger once again (200x265x30mm, vertical tube flow orientation), with 6 passes splitted into two rows configuration. This means that the exchanger has two rows of tubes along its depth, and each of them allows 3 flow passes, improving the heat exchange. This particular configuration has been selected considering the tests that needed to be carried out and similar cabin evaporators as well, tuning the layout so that the calibrated controls could reach the target in several operating conditions. The valves highlighted in blue in the map, *EV8* and *EV4*, are employed as expansion valves (*EXV*). Although GT-SUITE does already provide a standard template in the library for TXVs, their control strategy is rather simple, acting

on the opening area to target the fluid superheat in a specified circuit location. In this study case, the double evaporator configuration needs a more refined control strategy for the EXV opening areas. For this reason, a custom connection has been chosen, whose control strategy has been developed from the ground up and explained in *Section 3.3.3*.

To conclude this section, the switch system inserted just downstream and upstream of the compressor will be discussed. The idea behind those custom connections is the same of the already explained *EVA* and *EVB* valves in the cooling circuit. *EV3*, *EV14*, *EV15* and *EV16* are just connections that close when a certain layout of the circuit is required. *HP-switch1*, *HP-switch2*, *HP-switch3*, *HP-switch4* are, on the other hand, just *FlowSplit* templates used to model the valve volumes, whose inlets and outlets are managed by the linked custom connections. The purpose of the linking system is to invert the direction of the refrigerant towards the heat exchangers, while keeping the same direction across the compressor at the same time. If the refrigerant mode is required, *EV14* and *EV15* are open, *EV3* and *EV16* are closed, therefore the refrigerant goes through the exchangers at the top and condenses, and then evaporates. If the heat pump mode is required, *EV3* and *EV16* are open, *EV14* and *EV15* are closed. Therefore, the refrigerant condensate in the exchangers at the bottom, releasing heat to the battery or to the cabin, and the upper condensers are used as evaporators.

The different layouts and configurations explained in this section have been used to run battery cooling tests and cabin heating tests. The results of each test with the relative layout will be discussed in *Section 3.5* and *Chapter 4*.

3.3.2 Compressor controls

The compressor is responsible for the refrigerant flow rate in the HVAC circuit, on which the heat exchanged and the variations in temperature depend. This means that a control strategy is needed in order to generate the right amount of flow to reach the temperature targets. In *Figure 3.9* the developed controls acting on the compressor speed are shown.

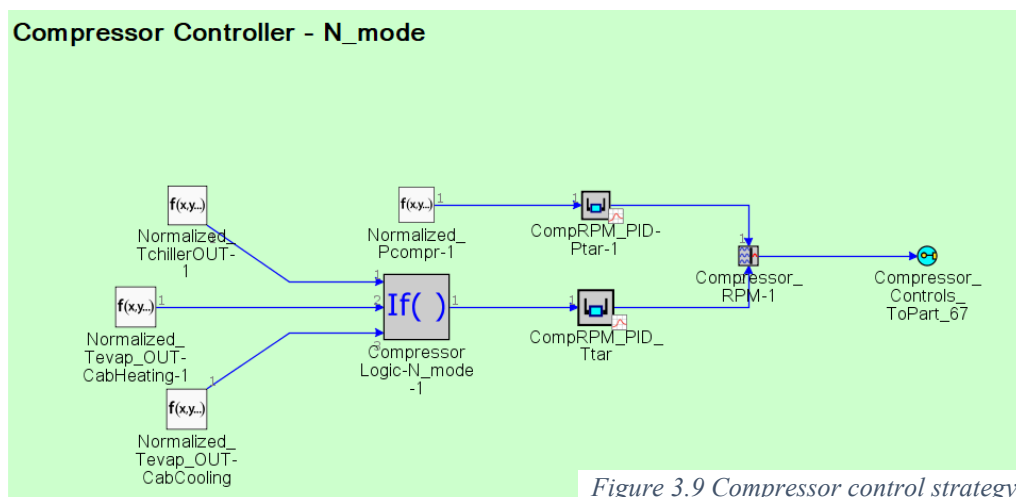


Figure 3.9 Compressor control strategy

The control is assigned to a PID Controller, which uses a feedback loop mechanism to evaluate the error between a variable and the target that has been set and tries to correct it by means of Proportional, Integrative and Derivative gains, hence the name. In this case, the gains have been calibrated iteratively and a target of 2 as been set. The PID has three possible input signals: chiller outlet coolant temperature, evaporator outlet air temperature in cooling and in heating. All signals are normalized to the target value of temperature, so that a single target can be set in the controller (*Equations 3.1*). In case of cabin heating, the input signal is the inverse of the normalized fraction, in order to make the PID behave in the same way in the three cases: an input signal bigger than 2 will make the compressor speed up, a signal lower than 2 will make the speed decrease. If the normalized signals were all the same, in case of heating, the PID would correct the error by acting on the speed in two different ways with respect to the cooling cases.

$$2 \frac{T_{chillerOUT}}{T_{tar}} ; \quad 2 \frac{T_{evapOUTcool}}{T_{tar}} ; \quad 2 \frac{T_{tar}}{T_{evapOUTheat}} \quad (3.1)$$

The *CompressorLogic* block is in charge of passing to the PID the input signal relative to the configuration the system is into. The *Table 3.2* clearly summarizes the passed signal depending on the cases.

CASE	PASSED SIGNAL
Cabin Heating + Battery cooling	Chiller temperature
AC off + Battery cooling	Chiller temperature
Cabin Cooling + Chiller off	Evaporator temperature
Cabin Cooling + Battery cooling	Chiller temp + Evaporator temp

Table 3.2 Compressor logic

The *Table 3.2* does not include the evaporator outlet air temperature in the heating case because in the tested configurations, the cabin is warmed up by the heat extracted from the battery circuit, that can be partially dissipated in the underhood condenser or can be increased by the electric heater, depending on the cases. The cabin heating-up with a non-active chiller can be managed only in heat pump mode, not included in this project.

As *Figure 3.9* shows, the RPM PID output is not directly passed to the compressor speed. As a matter of fact, while attempting to reach the temperature target, the PID could force a high value of speed that results in a pressure of the refrigerant at compressor outlet that goes beyond the saturation limit maximum pressure, causing unrealistic results. For this reason, a second PID is added to the strategy, this time targeting a maximum pressure at compressor outlet of 28bar.

Therefore, two values of compressor RPMs are calculated by the strategy, one needed to reach temperature targets, the other to reach a pressure of 28bar. The minimum signal

between the two is passed, so that as soon as the temperature targets are met with a value of speed that does result in an excessive pressure, the strategy switches to the value of speed that maintain the pressure at 28bar.

Also for the secondary PID the input is a normalized signal and it is multiplied by a factor of 2, so that the two PIDs are targeting the same value and there is no problem in switching.

3.3.3 Thermal Expansion Valves controls

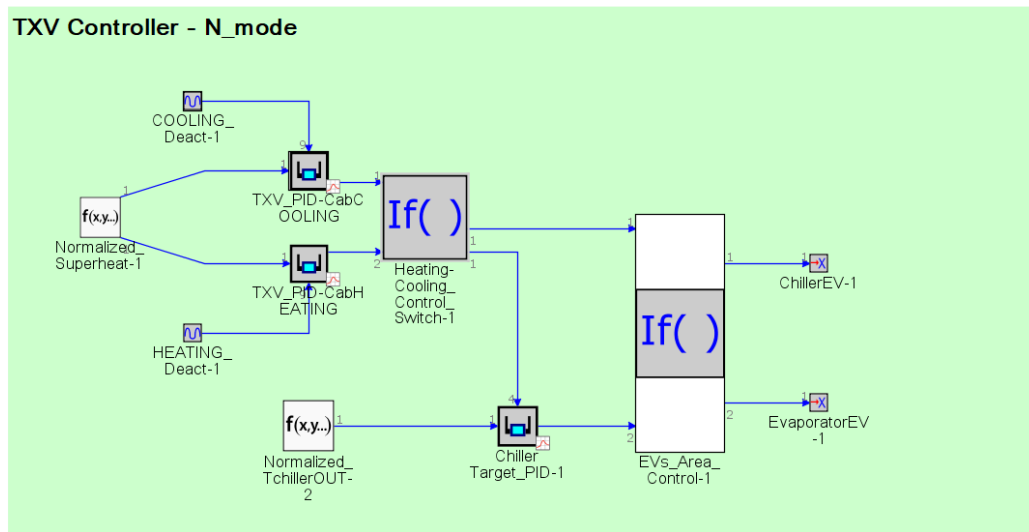


Figure 3.10 Expansion valves control strategy

In Figure 3.10 the developed strategy for the expansion valves (*EV4* and *EV8* in Figure 3.7) is shown. If the goal of the compressor control was to generate enough flow rate to allow the required heat exchange, in this case the objective is to reach a superheat value of 10K at compressor inlet. As a matter of fact, the normalized superheat is given as input signal to the two EXV PIDs, deactivated alternatively depending on the cabin being cooled down or heated up. The gains of the two PIDs have been calibrated to be able to meet the target robustly in different conditions, and in this purpose prospective 4 compressor speed-dependent maps have been generated, by tuning the relative gain at 3 compressor speeds (500, 3000, 7000 rpms) in each of the two cases. The derivative gain has been set to zero.

The PIDs calculates an equivalent EXV area that is needed to achieve 10K superheat. Their outputs are given to an *if* block that simply let through the signal depending on which PID is active. A third PID block receives as an input signal the chiller outlet coolant temperature, the same that enters the compressor control PID and it is needed in order to meet the target temperature of the battery coolant. The *EVs_Area_Control* block manages the three cases the circuit can work in, deciding the areas that have to be sent to the chiller side EV (*EV8*) and to the evaporator side EV (*EV4*).

If there is no AC request, then the equivalent EXV area is sent to *EV8* and the refrigerant evaporates in the chiller. If there is no need to cool down the battery, but the driver wants to cool down the cabin, then the equivalent EXV area is sent to *EV4* and the fluid evaporates in the cabin heat exchanger. In these two cases, the targets on temperature are met thanks to the control on the compressor speed. If both chiller and cabin evaporator are active, the equivalent area represents the total area needed for the expansion and it is split up between *EV8* and *EV4* in order to reach the temperature targets on the specific components. That's where the *ChillerTarget_PID* comes into play: once the equivalent area is found, it decides how much of that area is needed to reach the desired battery temperature; by subtraction the area for *EV4* is evaluated. So, to sum up, the compressor provides the total flow needed to satisfy both battery and cabin requirements, the EV logic evaluates the area needed to meet the superheat requirement and splits it up between the chiller and evaporator. *Table 3.3* schematizes the logic.

CASE	CHILLER EV	EVAPORATOR EV
Cabin Evaporator OFF	Equivalent TXV area	0
Cabin Evap ON + Chiller OFF	0	Equivalent TXV area
Cabin Evap ON + Chiller ON	Chiller PID area	Equivalent TXV area – Chiller PID area

Table 3.3 HVAC EV areas logic

Obviously, the area evaluated to reach the target on the battery is saturated by the total EXV equivalent area: in the worst case, all the fluid evaporates in the chiller, and *EV4* remains closed. Operating in this way, a priority of targets is introduced: the battery, which integrity is extremely temperature-sensitive, must be cooled down in every scenario; the cabin on the other hand has no problem to wait a little bit longer or to settle for a slightly different temperature it asked for.

Knowing the EV logic, it is also easy to understand why the compressor PID has been chosen to have as input signal the sum of the normalized chiller and evaporator temperatures in case they are both active. Even if it seems a 2 degrees of freedom equations, it comes to just one if there is another PID targeting one of the two signals.

3.4 Cabin circuit

The description of the cabin circuit concludes the discussion about the entire TMS model. A schematic of it can be seen in *Figure 3.11*.

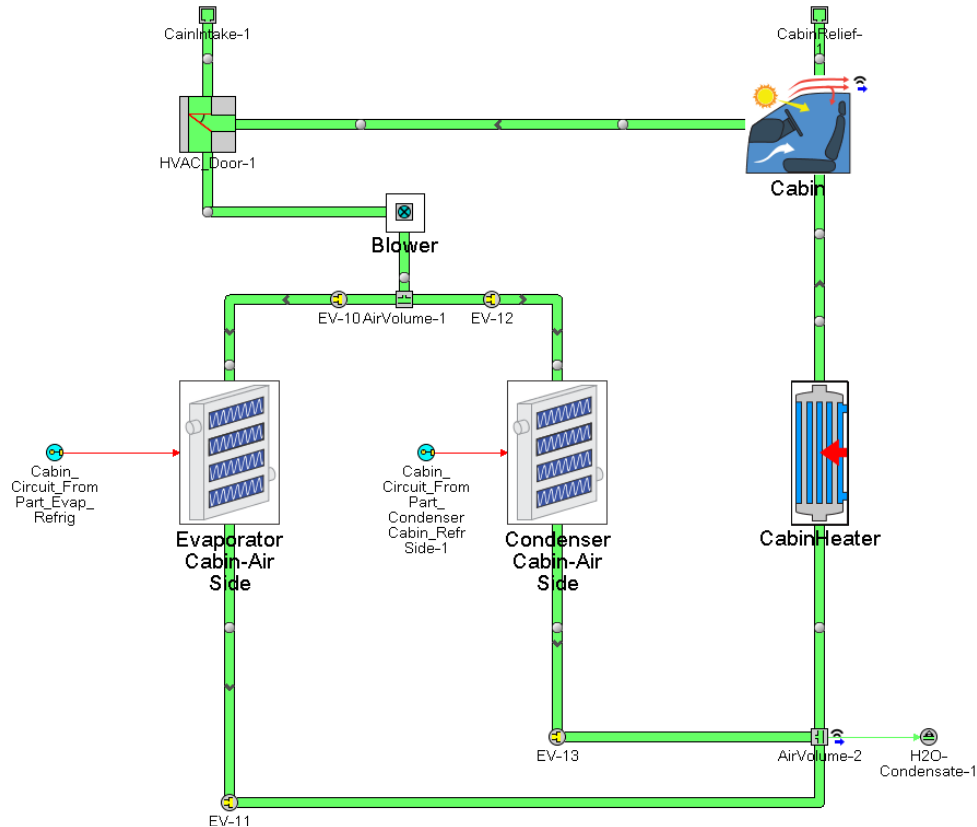


Figure 3.11 Cabin circuit

The two heat exchangers are the secondary templates of the cabin condenser and evaporator coupled with the HVAC circuit. The air passing through them is collected in a volume from which water condense is removed. Its temperature is the one targeted by the compressor controls, so that it can be used either if the cabin is being cooled down or heated up. In addition, the two exchangers can be isolated by the two custom connections at their inlet and outlets, in case one is not active. Moving downstream, an electric heater is modelled. It can be used in heating mode but also in cooling mode: in case the air gets cooled down more than necessary in order to remove humidity, the heater can bring the temperature back up. The cabin itself has been modelled with a standard GT-SUITE template and its pressure is imposed to be the atmospheric one. No solar flux radiation is considered in this study. The air enters in the circuits from the environment at 1bar through the vents: *HVAC_Door* templates allow to model them easily, giving to the user the possibility to close or open them. The task of generating flow rate is given to the blower, modelled as an electric fan (100mm blade diameter, 25mm hub diameter, 15mm blade depth). Usually, it is controlled in order to better manage the temperature reached in the cabin, but in this project it will be activated at constant speed. In *Figure 3.12*, its operating map can be seen.

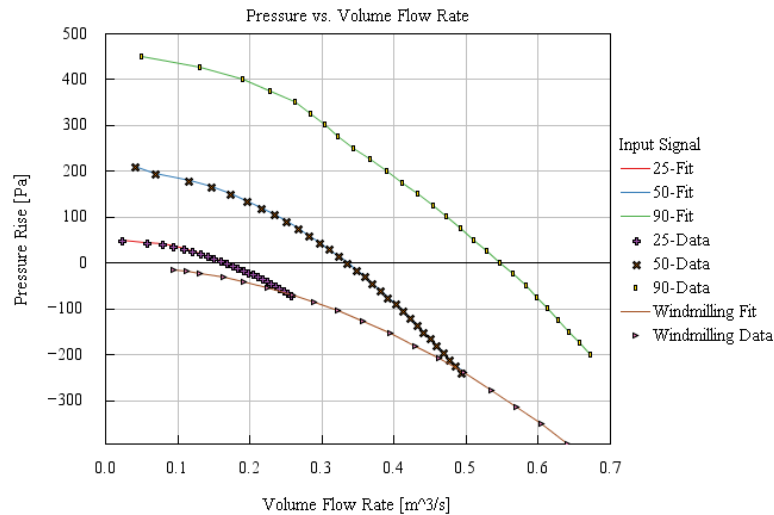


Figure 3.12 Blower working map

3.5 HVAC system sensitivity analysis

Once the model has been built, some sensitivity tests have been performed in order to verify the robustness of the system and of the control strategy. Two separate configurations have been used: battery cooling and cabin cooling. In the next sections the results will be discussed in detail.

3.5.1 Battery cooling – chiller mode

Looking at *Figure 3.2*, the coolant circuit configuration is the *blue* one, achieved by closing *EVA_switch-2* and *EVB_switch-2*. In this way, the heat rejected by DC/DC converter, inverter, electric motor and OBC is dissipated by the main radiator, the battery temperature on the other hand, is managed by the chiller. For what the HVAC circuit is concerned, the refrigeration mode is used and the connections to the cabin condenser and evaporator remain closed. Therefore, the compressed flow condensates in the underhood heat exchanger, gets expanded by *EV8*, and evaporates in the chiller before going back into the compressor and closing the loop. *Figure 3.13* gives an idea of the flow path, in red.

The cabin circuit will not be considered in the following tests, as no heat is exchanged with that circuit. The blower is still active but is kept to a minimum speed to allow air recirculation; no sensible temperature or pressure variation is recorded.

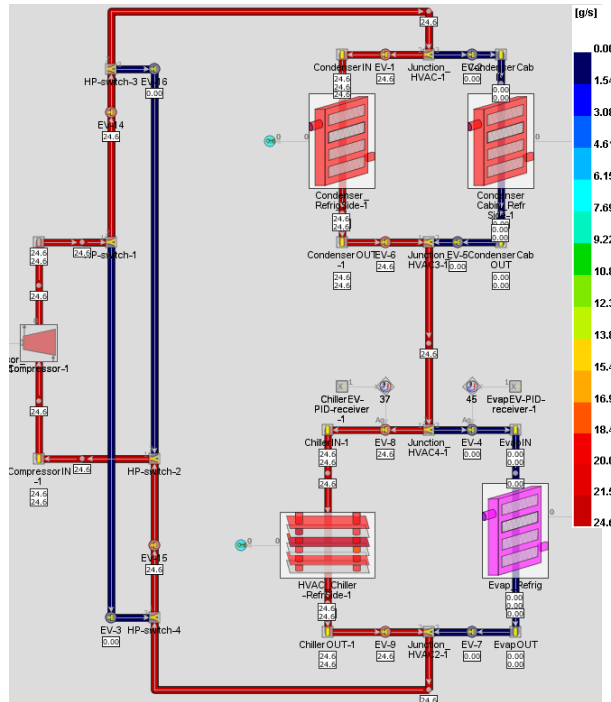


Figure 3.13 HVAC flow path

The main goal of this analysis is to understand how the battery temperature is managed by the HVAC circuit. For this reason, the test has been run performing a battery heat rejection sweep, 3000W, 3500W, 4000W, 4500W and 5000W. These values of heat rejection are actually quite severe. In addition, they are given as constants for the whole simulation duration (about 1000s), whilst in reality a battery pack will release those quantities of heat for significantly shorter periods of time. As a consequence, the sweep covers worst-case scenarios to find the limits of the system. All the other heat source are set to 0W, as they are managed by a separate circuit and would have slowed down the simulation.

The targets of the control strategy are 10K of superheat at compressor inlet and 25 °C of coolant at chiller outlet.

For what the boundary conditions are concerned, 23 °C of ambient temperature and 1bar of ambient pressure are used. The initial coolant temperature is set at 25 °C, so the system can be observed as it tries to maintain a safety margin while the battery keeps releasing heat into the fluid. To reduce the complexity of the circuit and to eliminate an extra variability factor, the coolant pumps are run in a speed of 4000rpm, in order to maximize the heat exchange in the battery water jackets.

The vehicle is set to be running at 50 km/h. Because of vehicle model unavailability, the power delivered by the battery is not linked to the car speed, therefore the choice of constant velocity can be justified considering the motion resistant forces to increase as the power delivered (and so heat rejection) increases. As a consequence, a roughly constant air flow through the condenser is expected cross the sweep. Its value is however increased in all cases by an active fan spinning at 2230rpm.

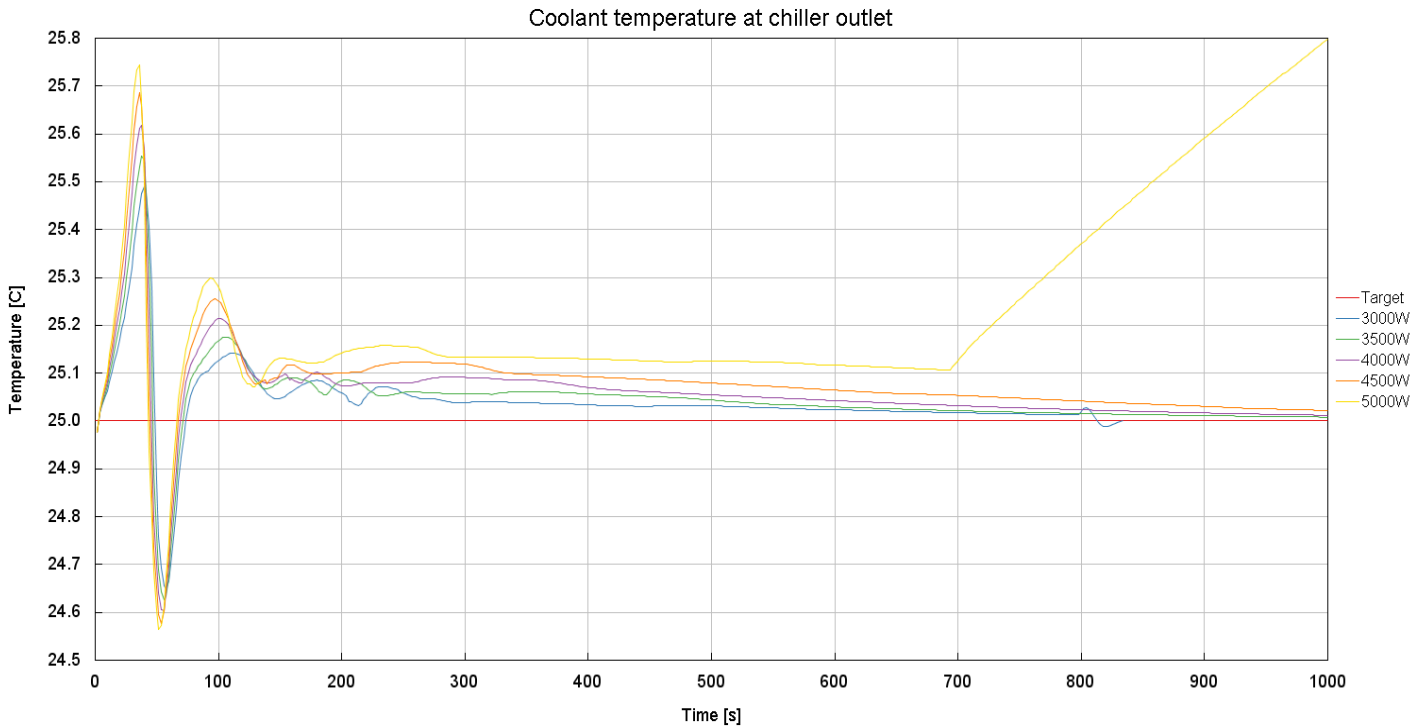


Figure 3.14 Chiller outlet temperatures

In *Figure 3.14* the chiller outlet coolant temperature can be seen for each case. Except for the 5000W case, they show a similar behaviour, starting off with a small overshoot, whose peak value increases as the heat rejection increases, and settling sooner or later on the 25 °C target. The 3000W case stops before the end of the simulation because the software registered the reach of the steady state. For the 5000W case, the trend is aligned with the other cases, but at about 700s the temperature starts to increase rapidly, showing that the system is no more able to dissipate that amount of heat. Such a behaviour is an indication of a system limit: the compressor, in fact, reaches its maximum speed, as it will be shown in *Figure 3.17*.

In *Figure 3.15*, the performance of the PID targeting the superheat can be analysed. It does not show any critical point, the target is reached in every case quite well. The initial overshoot is a bit high, but it doesn't compromise the compressor performance and does not affect the behaviour of the 5000W chiller temperature at 700s, shown in *Figure 3.14*. It can be concluded that the superheat PID works correctly, evaluating the needed flow area and passing it to *EV8*. *Figure 3.16* shows the area values for all the cases. It can be noticed that the trends are really similar, the only deviation could be highlighted on the 5000W curve, that at about 700s changes its slope quite abruptly. This is probably another consequence of the same problem causing the outlet chiller temperature to diverge from the target. Moreover, in *Figure 3.16*, a yellow horizontal line can be seen, corresponding to an area of about 0.05mm². It represents a minimum output value, needed so that the PID cannot force *EV8* to close too much and increase the resistance in the circuit, affecting negatively the flow rate. A similar limit is also introduced as maximum output, equal to the geometric area of the connected pipes of 314 mm². It is not shown in the plot because of the scale used.

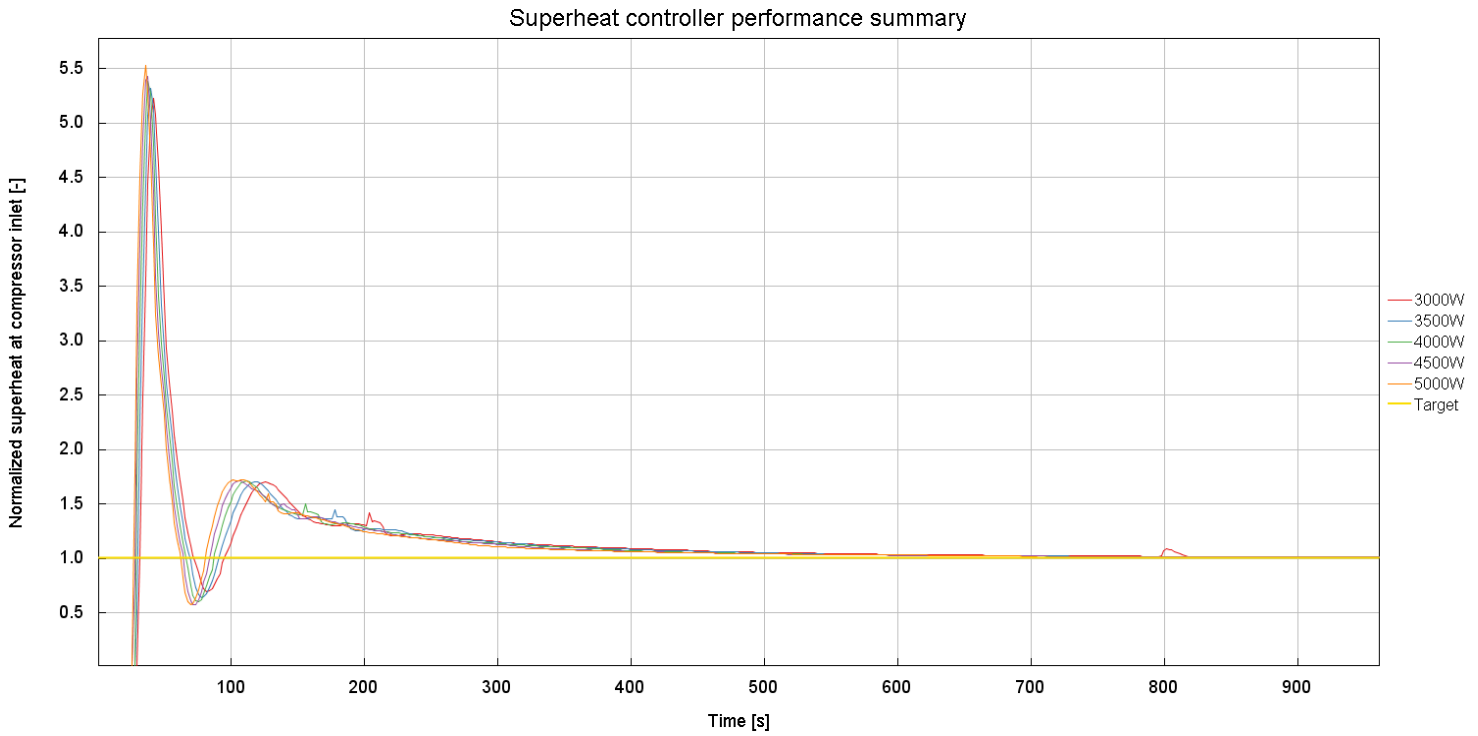


Figure 3.15 Performance summary of superheat PID

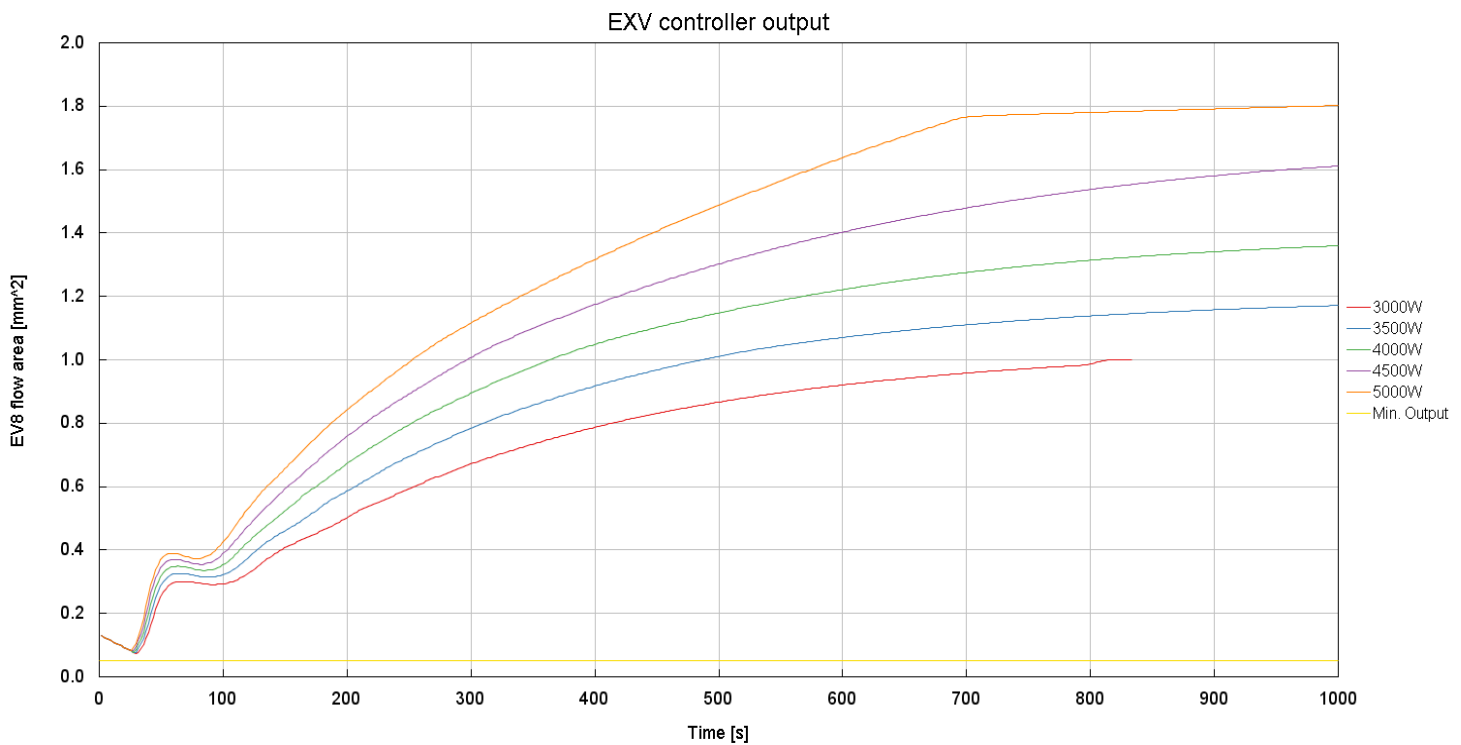


Figure 3.16 Superheat PID outputs

The compressor PID outputs give a clear idea on why the target is not met in the 5000W case (Figure 3.18).

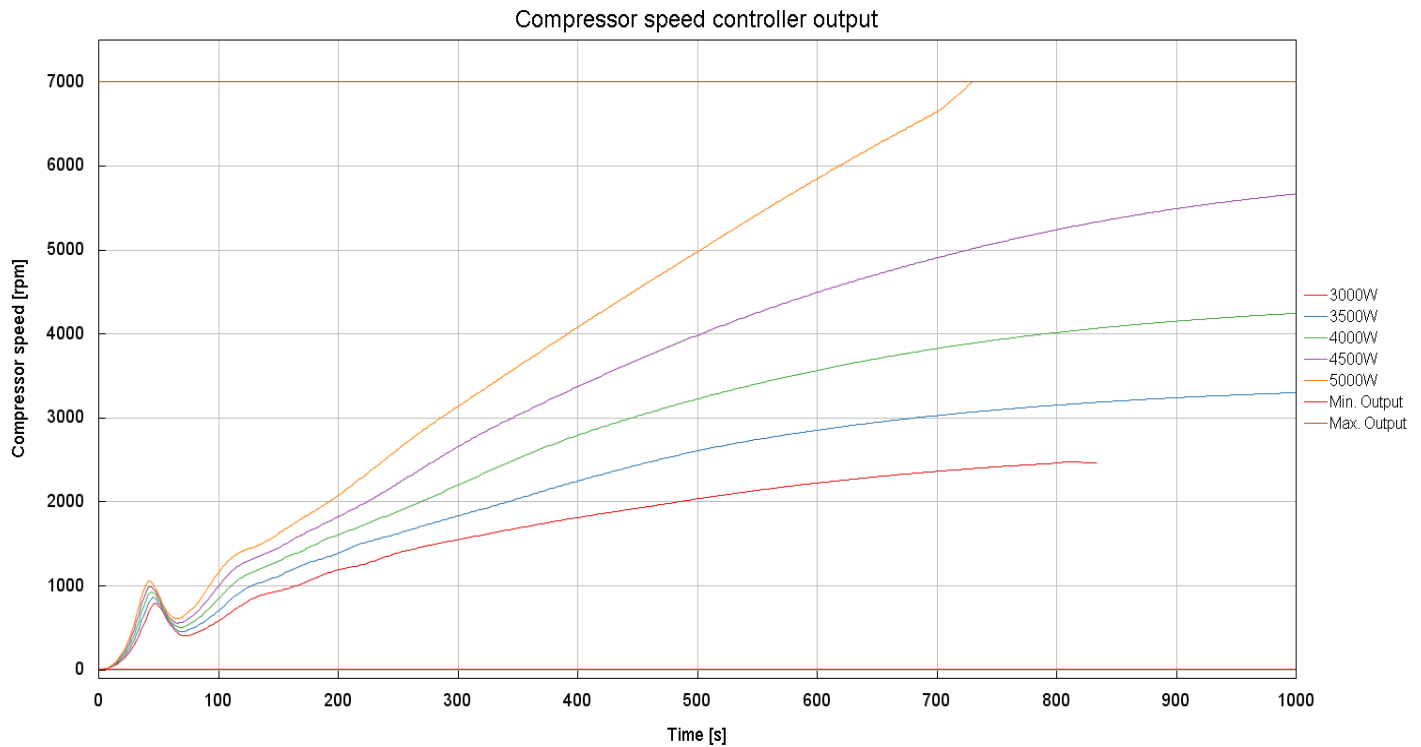


Figure 3.17 Compressor PID outputs

For 3000W, 3500W, 4000W and 4500W, the PID gives similar outputs in terms of trends. It starts by rapidly increasing the compressor speed, causing the temperatures (Figures 3.5) to drop quickly in the first 50 seconds. Once they get lower than the target, the PID tries to slow down the compressor, causing the temperatures to rise again. After 100s, the controller starts increasing the rpms again, this time in a slower and more progressive way. As the temperatures get close to the target, the speeds reach a plateau of about 2400rpm, 3300rpm, 4200rpm and 5600 rpm: to manage a more severe condition, the compressor has to spin more, as one would expect.

Conversely, for the 5000W case, the PID keeps increasing the compressor speed more or less linearly. This means that initially the system is already in a limit condition, in which the temperature can be managed only if the compressor has high rpms. As a matter of fact, the temperature decreases more slowly than the other cases, even if the rpms are higher in every instant. At about 700s the PID calculates that a speed higher than the maximum allowed by the component itself is needed, so it saturates at 7000rpm and the temperature consequently increases due to the heat that is not dissipated anymore.

In conclusion, the controller works quite well and tries to meet the target, but the system as it is designed cannot handle 5000W of heat rejection from the battery for prolonged periods of time. The PID gains could be furtherly refined, but the only result would be reaching the speed needed to satisfy the target earlier in the simulation at the cost of some initial instability. For the 5000W this means just reaching 7000rpm sooner, but since an higher speed is needed, the temperature will not reach the target anyway.

3.5.2 Cabin cooling – evaporator mode

For cabin cooling testing, the circuit configurations to take into account are the HVAC, the cabin and the underhood ones. The coolant circuit does not contribute to the cabin cooling in the performed tests. *Figure 3.18* shows the flow path (in red) in the HVAC circuit.

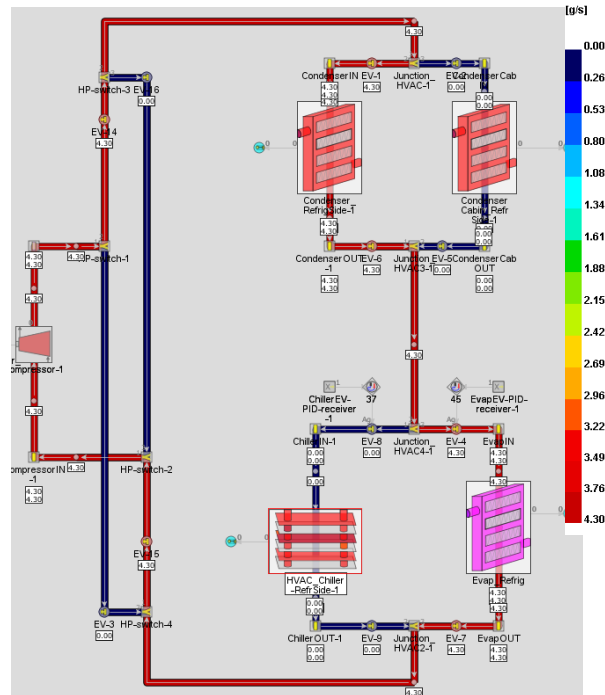


Figure 3.18 HVAC flow path

The active condenser is again the underhood one, since the cabin has to be cooled down. The connections with the chiller (and so with the coolant circuit) *EV8* and *EV9* are closed, and all the refrigerant expands and evaporates in the cabin heat exchanger, absorbing heat from the cabin circuit. On the air side, the connections with the condenser are closed, so that the mass flow rate taken from the environment can release heat to the refrigerant and eventually absorb heat from the cabin. Although the electric heater could be employed to reach the desired temperature requested by the passengers whilst the controller targets the evaporator outlet temperature, the focus of the performed test is to evaluate the correct functioning of the control strategy, so it will be kept off. The blower is commanded at medium/high speeds, at about 80% of its capacity, so that no cabin-side bottlenecks in the heat exchange process can occur.

Figure 3.19 shows the layout of the cabin air circuit, highlighting in red the flow path.

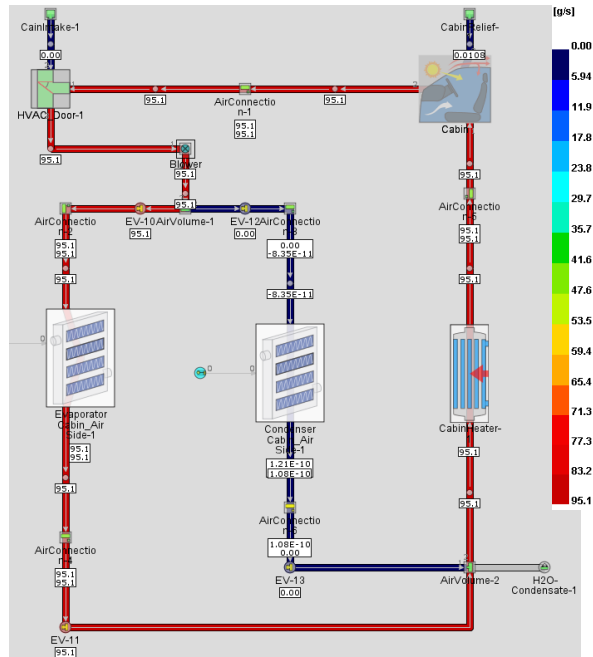


Figure 3.19 Cabin circuit flow path

The analysis has been performed to understand how the system adapts under different external conditions to provide enough cabin cooling. For this reason, it has been carried out with an ambient temperature sweep, 25°C, 30°C, 35°C, 40°C, 45°C, 50°C. They are quite representative values of hot season conditions, spanning up to the most severe ones. No other heat sources have been considered, as they are all disconnected from the studied configuration.

The targets regard a 10K superheat value at the compressor inlet and a temperature of 15 °C of air at evaporator outlet.

The initial conditions of the refrigerant have been set to 25°C for the first two cases, 30°C for the second ones and 35 °C for the last two and 1bar of ambient pressure.

The vehicle is considered to be moving at 50 km/h independently from the case, so a roughly constant flow rate is expected, taking also into account the radiator pack fan being controlled at constant speed of 2230rpm, to avoid bottlenecks in the underhood side of the model.

In *Figure 3.20* the temperatures of the air at evaporator outlets can be seen. The chart shows a really good calibration of the PID controller gains, as the targets are reached quite early in the simulation and no major variations can be noticed from 100s on for every case. High oscillations are not recorded either, the initial big drop can be explained by looking at the compressor speeds that the controller give as output (*Figure 3.21*).

As the simulation starts, the PID sees a big gap between the temperatures and 15°C goal. For this reason, the compressor is forced to go almost instantaneously to maximum speed to try and reach the target.

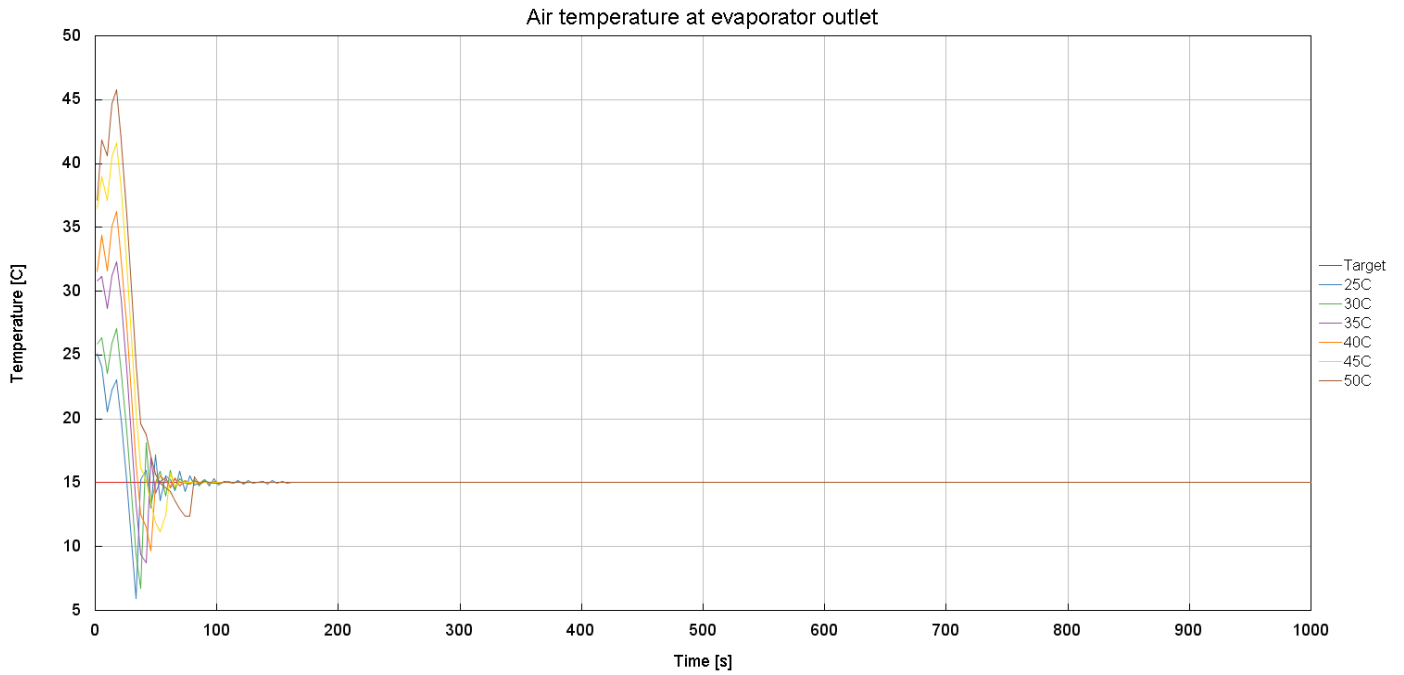


Figure 3.20 Evaporator outlet temperatures

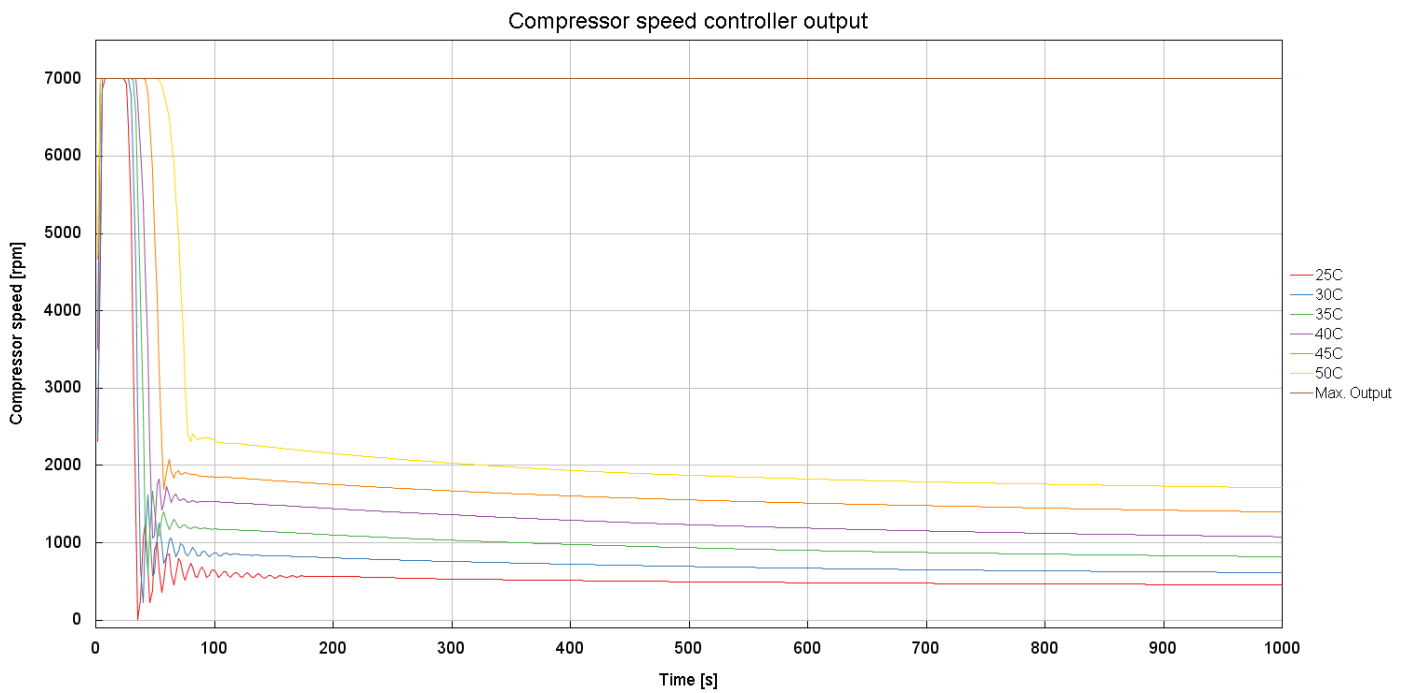


Figure 3.21 Compressor PID outputs

Once the temperatures approach 15 °C, the rpms are brought back to an intermediate value and stabilize with more or less oscillations, depending on the case. The biggest oscillations are in the orders of 500rpms; an acceptable compromise to a such responsive system, also considering the quickness of the rpms to reach a constant value.

Even in the most severe case, 50°C, the PID output chart shows that the compressor speed remains lower than 2000rpm, suggesting that the system is capable of higher performance or that there is room to downsize certain components.

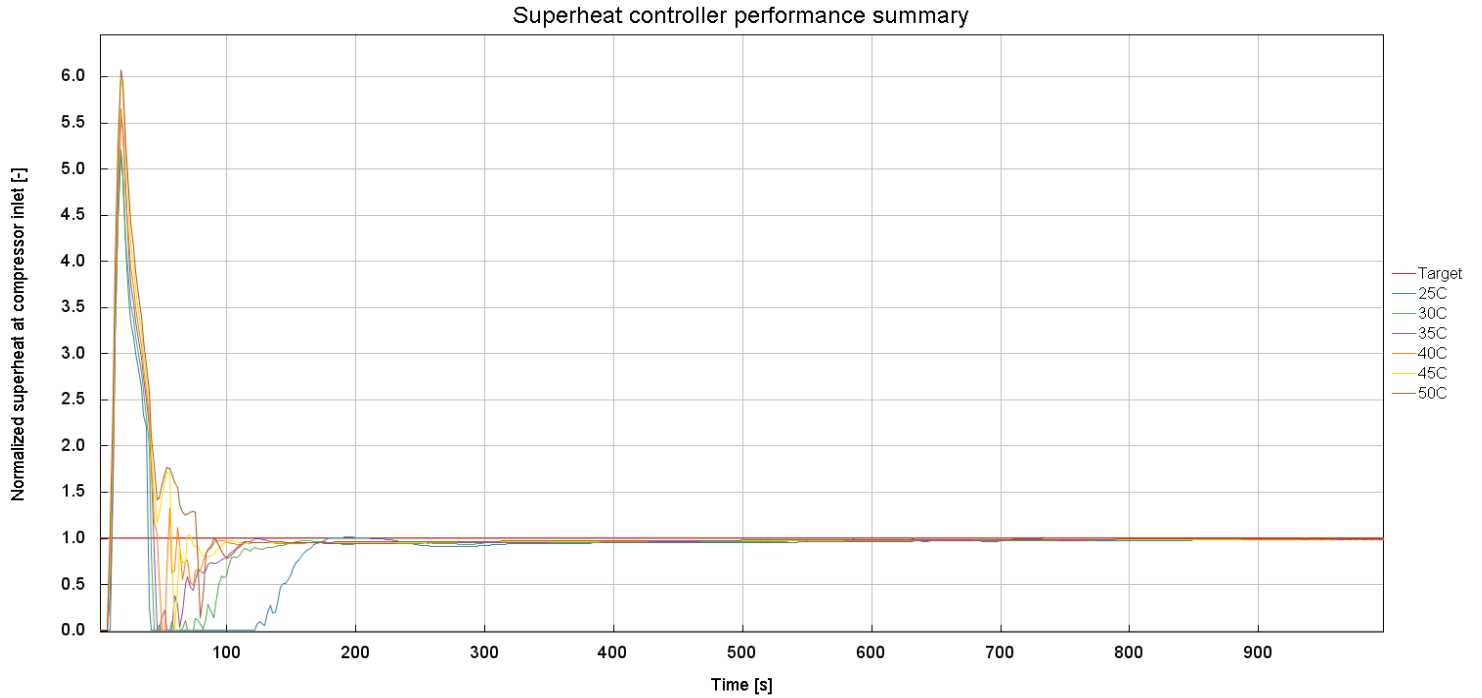


Figure 3.22 Performance summary of superheat PID

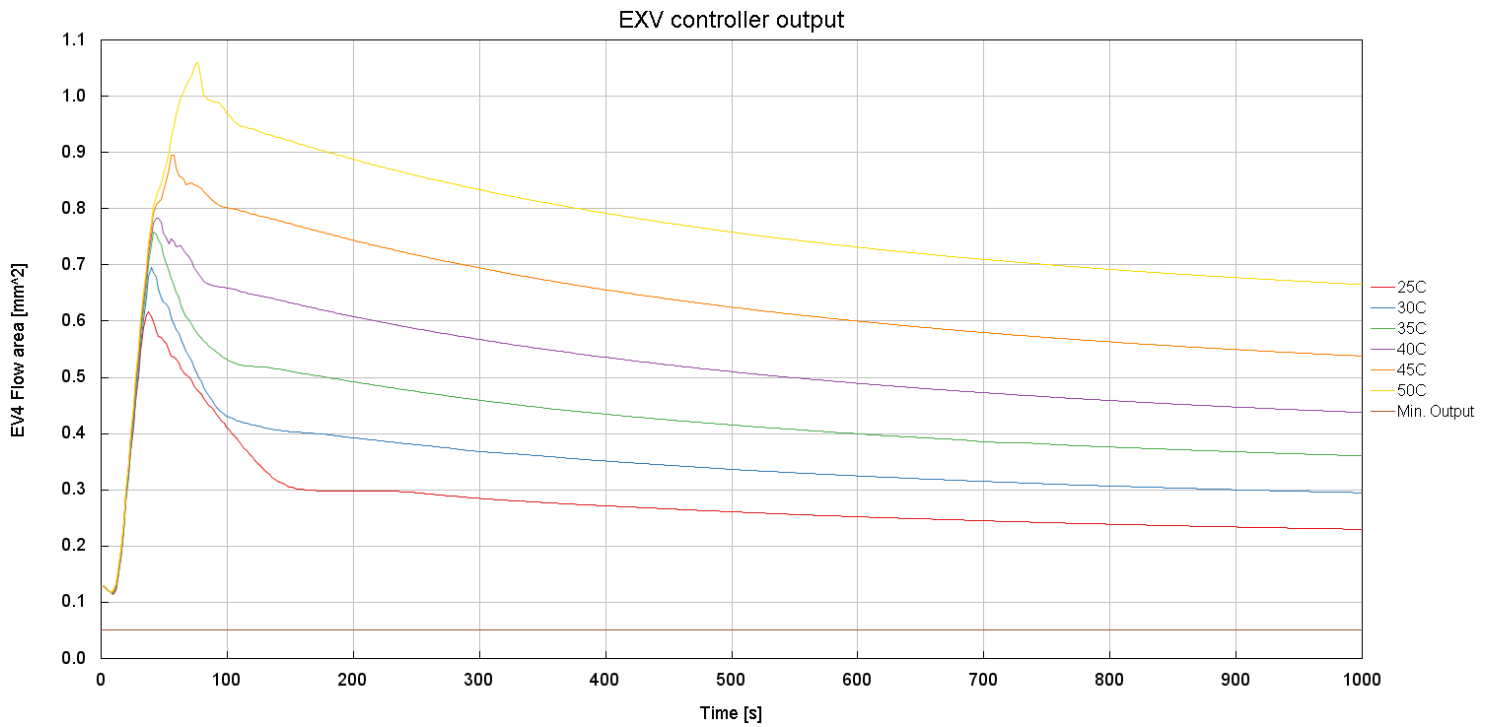


Figure 3.23 Superheat PID outputs

Also the superheat targets are reached quite well by the relative PID controller. For all cases an overshoot is recorded, but it does not compromise the integrity of the compressor. Moreover, a slight delay in reaching the target can be noticed for the 25 °C cases.

In conclusion, the ambient temperature sweep test shows an overall good behaviour of the cabin cooling control strategy. The targets, both in terms of temperature and superheat, are reached in a reasonable way in all cases, with no relevant oscillations or issues. The compressor manages to keep temperatures down without the need of an excessive speed and also *EV4* is controlled in a similar way across the sweep (*Figure 3.23*).

The two sweeps of battery heat rejection and ambient temperature have been useful to understand and validate the control strategies for the two configurations, a complete testing of both will be presented in *Chapter 4*, so that the critical operating points can be identified.

Chapter 4

Model applications

The model built for this project has been discussed in detail and tested to verify its capabilities. The purpose of this section is to demonstrate how it can be used in the development of a generic BEV. The applications that will be presented in the following concern:

- Critical operational points identification – Chiller and evaporator mode
- HVAC components selection
- Cabin heating strategy to optimize energy consumption

4.1 Critical operational points identification

One of the possible applications of the model is to evaluate the performance of the HVAC system, understanding its limitations and in what conditions they are reached. For this reason, the most demanding configuration has been tested, forcing the control strategy to manage both the battery temperature and the cabin cooling requests. The refrigerant mode is the one used. The refrigerant condenses in the underhood condenser and evaporates in both chiller and cabin, so that heat can be extracted from the coolant and cabin air circuits (*Figure 4.1*). The quantity of flow through the two evaporators, and in turn the quantity of cooling in the cabin and in the battery, is determined by the HVAC control strategy that takes into account the superheat requirements, whereas the compressor speed is calculated to meet both battery and cabin temperature targets.

The layouts of the different circuits are the ones already described in *Chapter 3*, referring to the cooling configurations. The coolant flow path is the blue one (*Figure 3.2*), so the radiator and battery circuits are independent from one another. On the cabin side, the connections with the condenser (*EV12* and *EV13*, *Figure 3.12*) are closed.

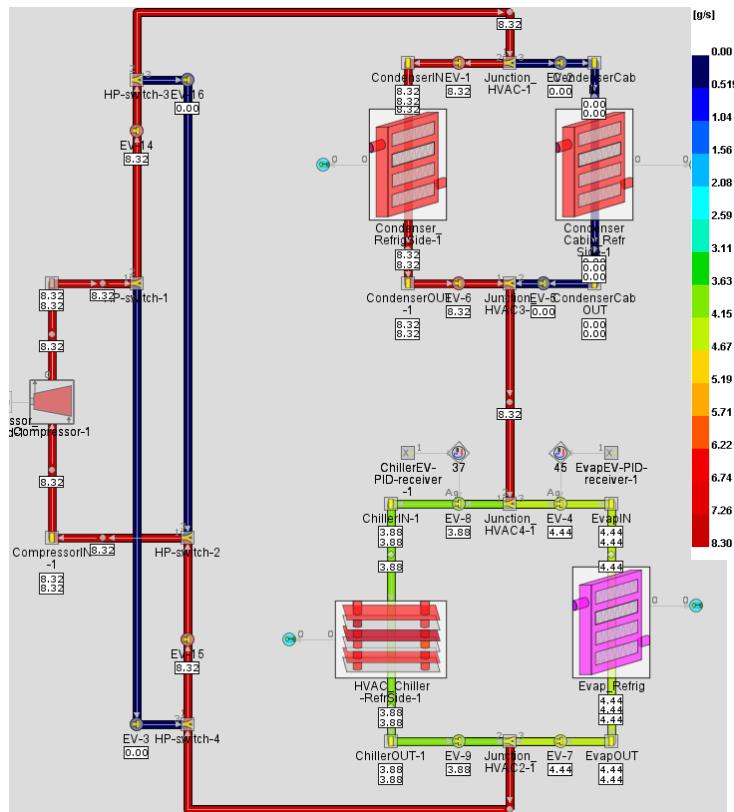


Figure 4.1 Full configuration flow path

Figure 4.1 is taken from one of the simulated cases, and it is clear that the control strategy splits the flow rate between the chiller and the cabin evaporator: the initial 8.32 g/s produced by the compressor is split in about 46/54% percentage by the opening of the *EV8* and *EV4* valves areas.

The simulation is set up to perform a DoE run. The Design of Experiment (*DoE*) is a useful tool GT-SUITE provides, that allow the user to carry out simulations in which systems have to be tested under several conditions or with numerous different parameters. This means that, instead of creating a lot of cases to change parameters' value manually, a DoE can be set up selecting the variables of interest and specifying the range of the sweep needed. Multiple cases are generated with all possible combinations of the selected sweeps, creating a single big simulation setup that will be run. For the identification of critical operating point, since the focus is on the HVAC system, two variables are included in the DoE setup:

- Ambient temperature: 25 °C to 50 °C (Step: 5°C)
- Battery heat rejection: 500W + 1000W to 5000W (Step: 1000W)

In total, 6 temperature values and 6 heat rejection quantities are combined in 36 cases, among which the limitations of the circuit can be found.

The others boundary conditions are pretty similar to the ones used in the validations described in *Sections 3.5.1* and *3.5.2*. The targets remain at 25°C for the battery coolant,

15 °C for the air at cabin evaporator outlet and 10K of superheat at compressor inlet. The vehicle is running at 50 km/h independently from the power lost (and generated) by the battery and coolant and refrigerant are both initialized at a temperature of 28°C. No heat rejection is imposed on the other sources managed by the main radiator.

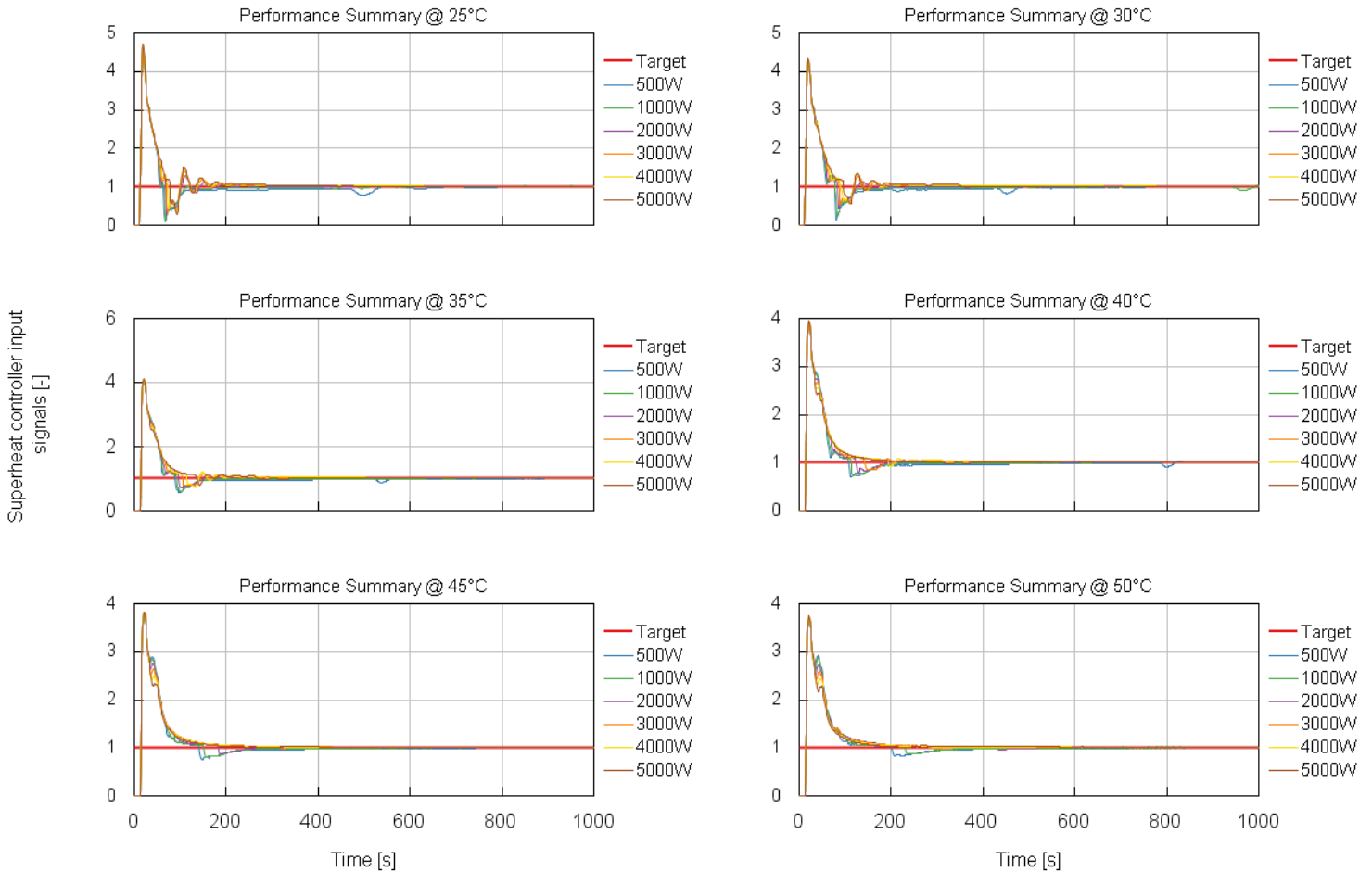


Figure 4.2 Performance summary of superheat PID

Figure 4.2 shows the input signals of the PID controlling the expansion valves area to achieve the superheat target, grouped by ambient temperature. The controller shows a really good behaviour in all the analysed conditions. The compressor inlet superheat reaches the target after an initial overshoot rather quickly, with an increasing stability as the temperature gets higher. The low-amplitude oscillations that can be noticed at lower temperatures, could be probably solved with higher proportional and integral gains, but the performance of the controller at higher ones would be compromised. As the behaviour of the superheat at 25/30/35 °C is reasonable anyway, it can be concluded that a good gains trade-off has been found.

It is quite interesting to notice that the area coming out from the superheat PID controller, is not directly passed to one of the expansion valves (*EV8* or *EV4*). The PID output is just a theoretical area that gets splitted between the two valves by means of the logic already explained in Section 3.3: the additional chiller PID evaluates how much of

the equivalent area is needed to achieve the battery temperature chiller, the rest is passed to the valve expanding the flow into the cabin evaporator. Therefore, in the analysed configuration, both expansion valves are active and the *Figure 4.2* shows that what counts is the total area of expansion and not how that area is achieved physically.

In order to better clarify how the additional PID works, two cases of the simulation are provided in *Figure 4.3* as an example.

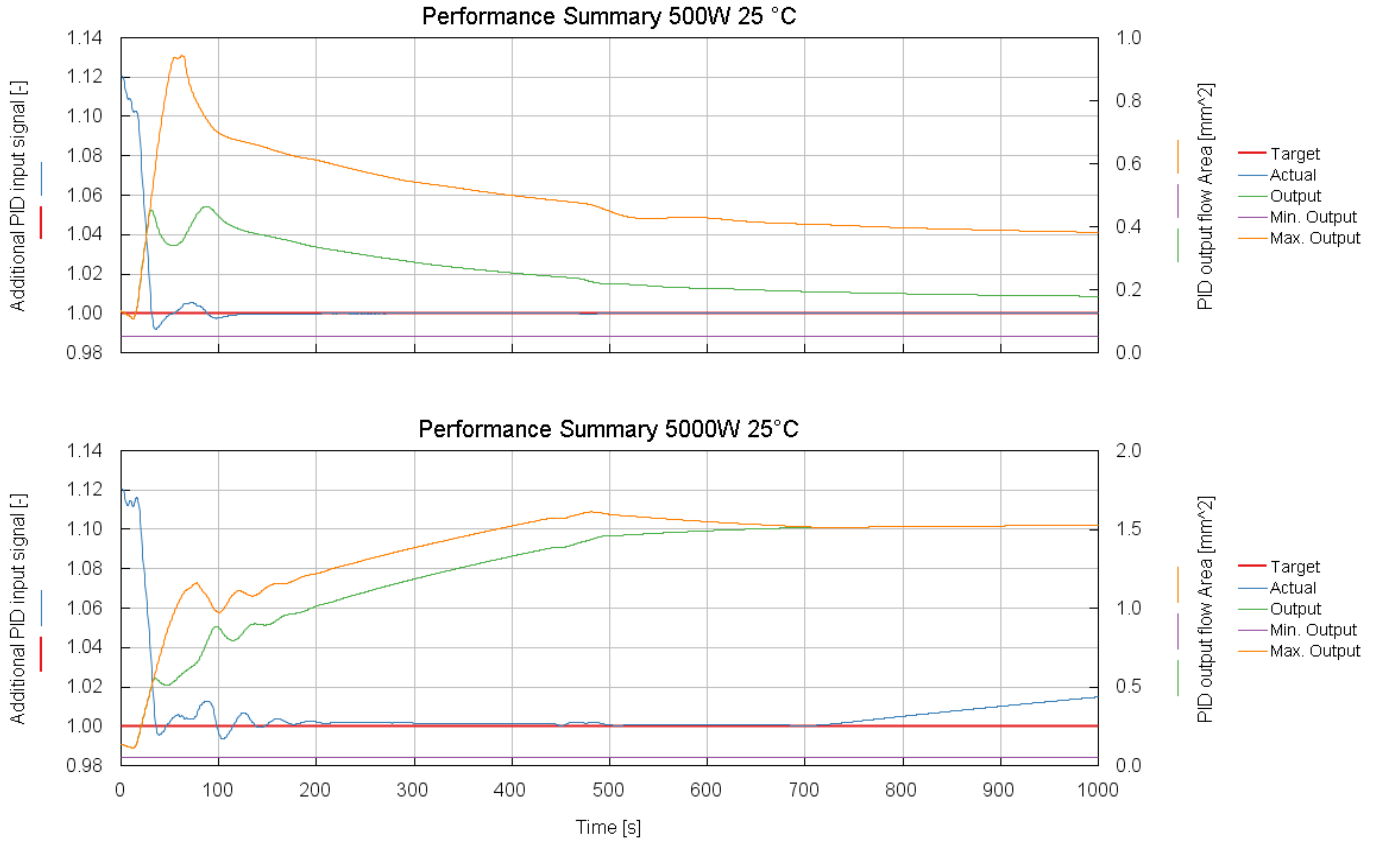


Figure 4.3 Additional PID performance summary

Two operating points at 25°C with a battery heat rejection of 500W and 5000W are shown, in the first case the temperature target is achieved, in the second one the battery coolant temperature diverges at about 750s.

Making reference to *Figure 4.3*, the target is shown in red as a horizontal line at 1, since the input signal (in blue) is normalized. The green and orange lines are respectively the PID output and the maximum allowed output, the latter being the area calculated by the superheat controller. Without considering the mass flow rate generation for the moment, which has a big role in reaching the temperature target anyway, it is evident how the additional controller works. For about 40s, the area that it evaluates is the maximum allowed because the actual temperature of the battery coolant is far from the target, so the logic wants to divert all the flow to the chiller, leaving closed the connection to the cabin evaporator. Once the temperature does get lower, the controller understands how much of the flow generated by the compressor (that already takes into account the target on the cabin side as well) is needed for the chiller and starts closing the relative valve.

That's why the additional PID output is an intermediate value between zero and the area needed to achieve the superheat target, as long as the temperature of the battery stays on the target as well. In the 5000W case, the additional PID understands that, from 500 seconds on, the flow on the chiller is not enough to absorb that quantity of heat, so it tries to open *EV8* even if the area coming from the superheat PID is slightly decreasing. At about 700s, the flow area needed to reach the temperature targets gets higher than the one needed to achieve the superheat target, so it saturates and the temperatures starts increasing once again. At the end of the simulation the target on the superheat (which has the priority to preserve the component) is met (*Figure 4.2*), whereas the one on the battery temperature is not, together with the target set at cabin evaporator outlet since no flow is left to expand into that heat exchanger. Therefore, 5000W of battery heat dissipation at 25°C is a critical operating point, and the system needs to be changed to be able to work in those conditions. Selecting a bigger compressor or an heat exchanger with a different layout could be a solution, but a lot of considerations have to be made regarding costs, packaging limitations and so on.

Other critical working points can be identified by looking at the compressor PID performance summaries (*Figure 4.4*). The input signals for each case can be analysed, as they are grouped together by ambient temperature.

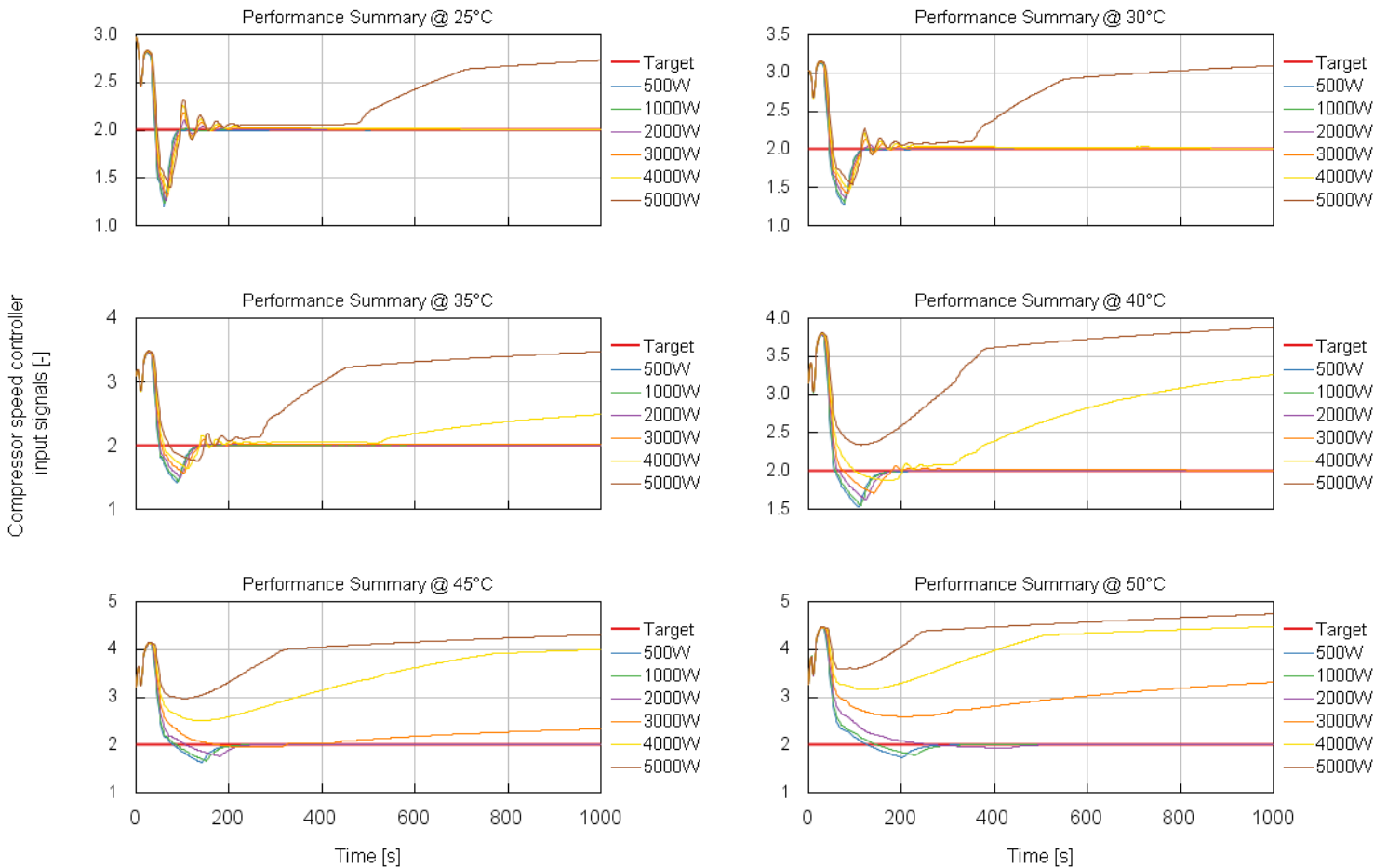


Figure 4.4 Performance summary of compressor PID

As one would expect, the system performance gets lower as the conditions get more demanding. The case that seems to be always beyond the capabilities of the circuit is 5000W, across a wide range of ambient temperatures. 500W, 1000W, 2000W of heat rejection are well-managed, even if they show progressively more oscillations for a specific value of temperature. Higher heat rejections on the other hand, are handled at relatively low ambient temperatures (25-30°C). At 35°C the target in the 4000W case is reached for about half of the simulation, then it starts to diverge and the system cannot dissipate enough such quantity of heat as the external conditions get worse. At higher ambient temperatures also 3000W become problematic and neither the battery nor the cabin can meet the required targets. Table 4.1 gives a clear idea about the cases in which the targets are met or not.

	25°C	30°C	35°C	40°C	45°C	50°C
500W	✓	✓	✓	✓	✓	✓
1000W	✓	✓	✓	✓	✓	✓
2000W	✓	✓	✓	✓	✓	✓
3000W	✓	✓	✓	✓	✗	✗
4000W	✓	✓	✗	✗	✗	✗
5000W	✗	✗	✗	✗	✗	✗

Table 4.1 Targets achievement summary

As a matter of fact, the target can be noticed to be 2, even if the temperatures coming into the PID as input signals are normalized. As already explained in *Section 3.3.2* (*Table 3.2*), for the case in which both chiller and cabin evaporator are active, the target of the compressor controller is the sum of the temperature signals normalized with their targets. Even if it seems to be an equation without a unique solution (e.g. ratios of 1.5 and 0.5 would still give 2 but the single temperature targets would not be achieved), the target on the battery coolant is also managed by the additional PID in the HVAC areas control strategy, so if the input signal goes to 2, it means that the single ratios go to 1.

For what the compressor speeds are concerned, it is easy to expect them to stabilize on a final constant value when the targets are achieved, and to go to the maximum allowed when the temperatures diverge. *Figure 4.5* shows their trends for the cases at 25 °C. The compressor is initially forced to speed up to produce a lot of flow and close the gap between the actual temperatures and the target. After some oscillations that vary with the case, the speeds reach a constant value depending on the amount of heat to dissipate. For the 5000W, since it has been already identified as a critical point, the compressor goes to maximum speed, but the temperatures cannot be kept under control.

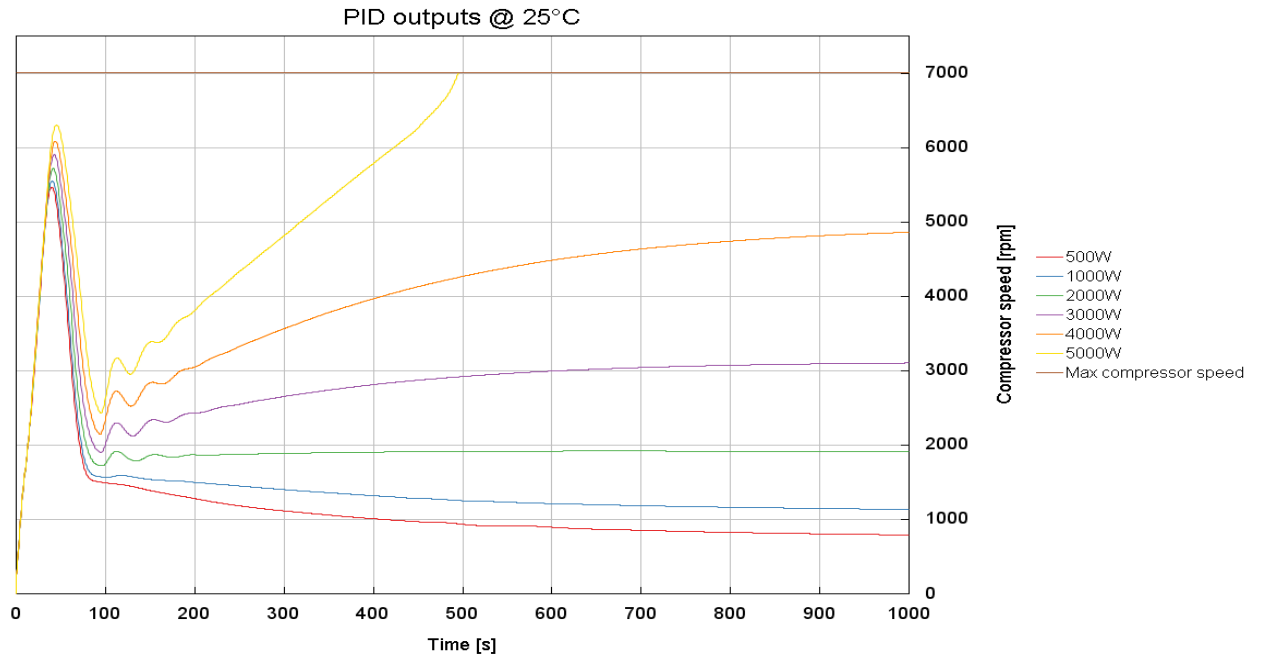


Figure 4.5 Compressor speeds at 25 °C

It has to be underlined however, that the heat rejections are given to the model as parameters, so they are constant throughout the simulation and do not affect other factors, such as the vehicle speed that in reality would have a higher air flow rate on the condenser as a consequence. Therefore, all the identified critical points could be managed by the chosen system to a certain extent, as the quantity of heat released by the battery could go that high for significantly shorter periods of time. A more realistic simulation would require a vehicle model, but it is not the case of this project.

4.2 HVAC components selection

The model described in *Chapter 3*, can also be employed to select some components with certain specifications. In the following, an example is given considering the underhood condenser as the component to be selected.

Referring to *Section 4.1*, one of the identified critical points is chosen, with the purpose of replacing the underhood condenser so that the temperature targets can be achieved. It has been already shown how the target on the superheat value is always achieved, so now the focus is shifted on the compressor controller and its output.

The selected working point is the one with 3000W of battery heat rejection at 45 °C. The performance summary of the compressor PID is shown in *Figure 4.6*.

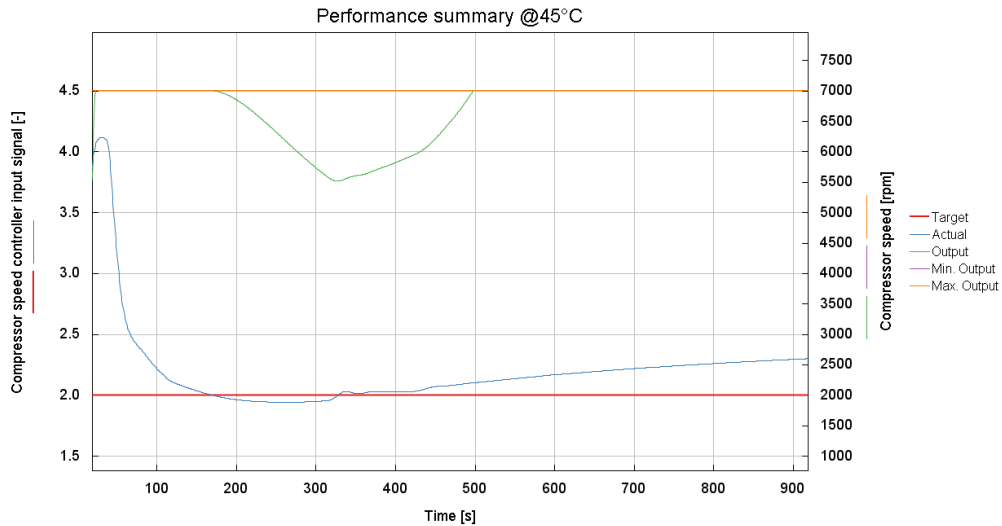


Figure 4.6 Performance summary of compressor PID

As it can be seen in the chart, the input signal containing both the coolant temperature at chiller outlet and the air temperature at evaporator outlet are on target for about 100s, but eventually diverges to almost 2.4. The output, on the other hand, goes almost instantaneously to the maximum to try and close the gap with the target. This causes the HVAC circuit pressure to rise quickly and reach dangerous levels, and so the pressure controller comes into play.

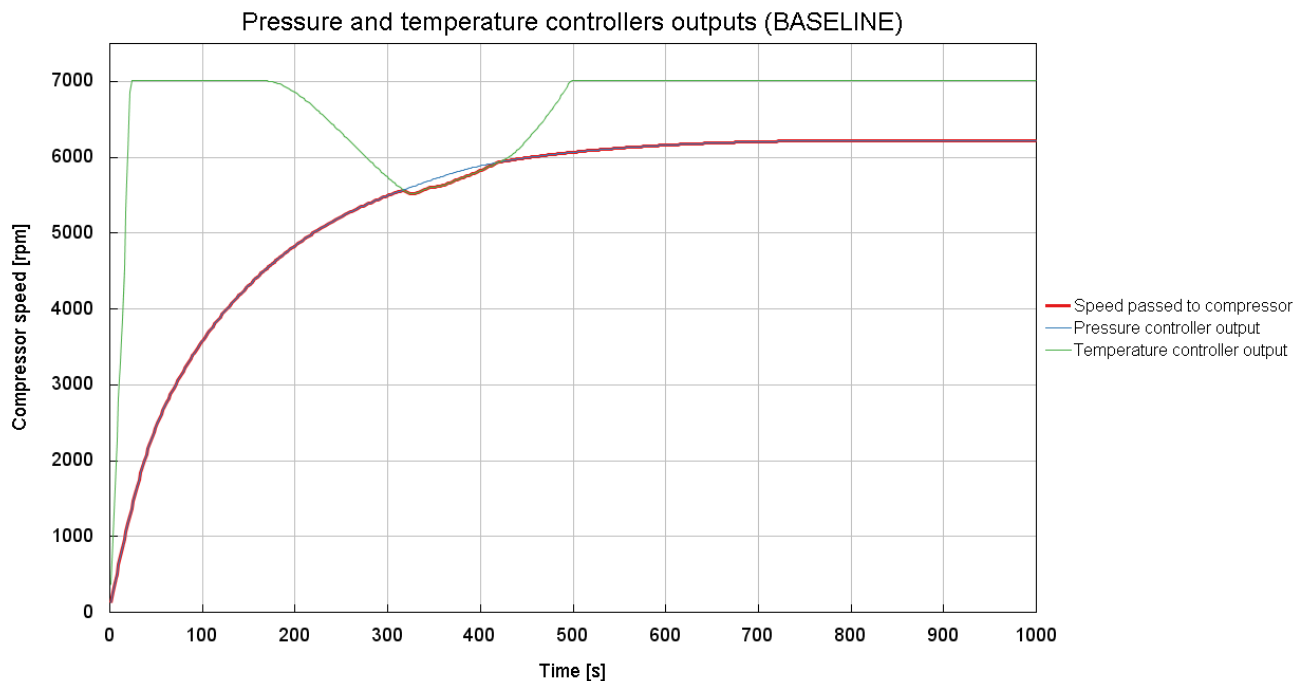


Figure 4.6 Compressor speed control (BASELINE)

Figure 4.6 shows the actual speed passed to the compressor (thick red line) versus the speed calculated by the PID controllers. It is evident how the temperature controller wants to crank the compressor up straight from the start, but to ensure a reasonable value of the pressure, the speed evaluated by the pressure controlled is passed pretty much during the entire simulation. The only exception is between 350s and 450s, where

the speed needed to achieve the temperature targets is lower than the speed needed to reach the pressure target, but as soon as the input signal rises again, so does the temperature PID output. The case taken in exam is therefore pressure-limited, but the bottom line is that one or both temperature targets are not reached, so the system needs to be improved.

Thanks to the possibility that GT-SUITE provides to scale a component along one of its dimensions, 5 different configurations of the underhood condenser have been tested, increasing each time its transversal dimension to improve the air flow area and the heat exchanged as a consequence. Starting off with a baseline tube length of 550mm, the configurations include: +10%, +20%, +30%, +40%, +50%.

All the other boundary conditions are the same already described in *Section 4.1*, so direct reference is made.

Figure 4.7 shows the temperature PID controller across the six considered cases. A remarkable improvement can be already seen in the configuration with +10% of tube length. The target is reached and maintained up to 700s, then the pressure controller output is passed to the compressor, similarly to the baseline presented in *Figure 4.6*. From the case +20% on, the situation gets progressively better. Any of the +30%, +40%, +50% configuration allows the target to be reached; usually the smallest one should be chosen, but other factors could affect the selection process.

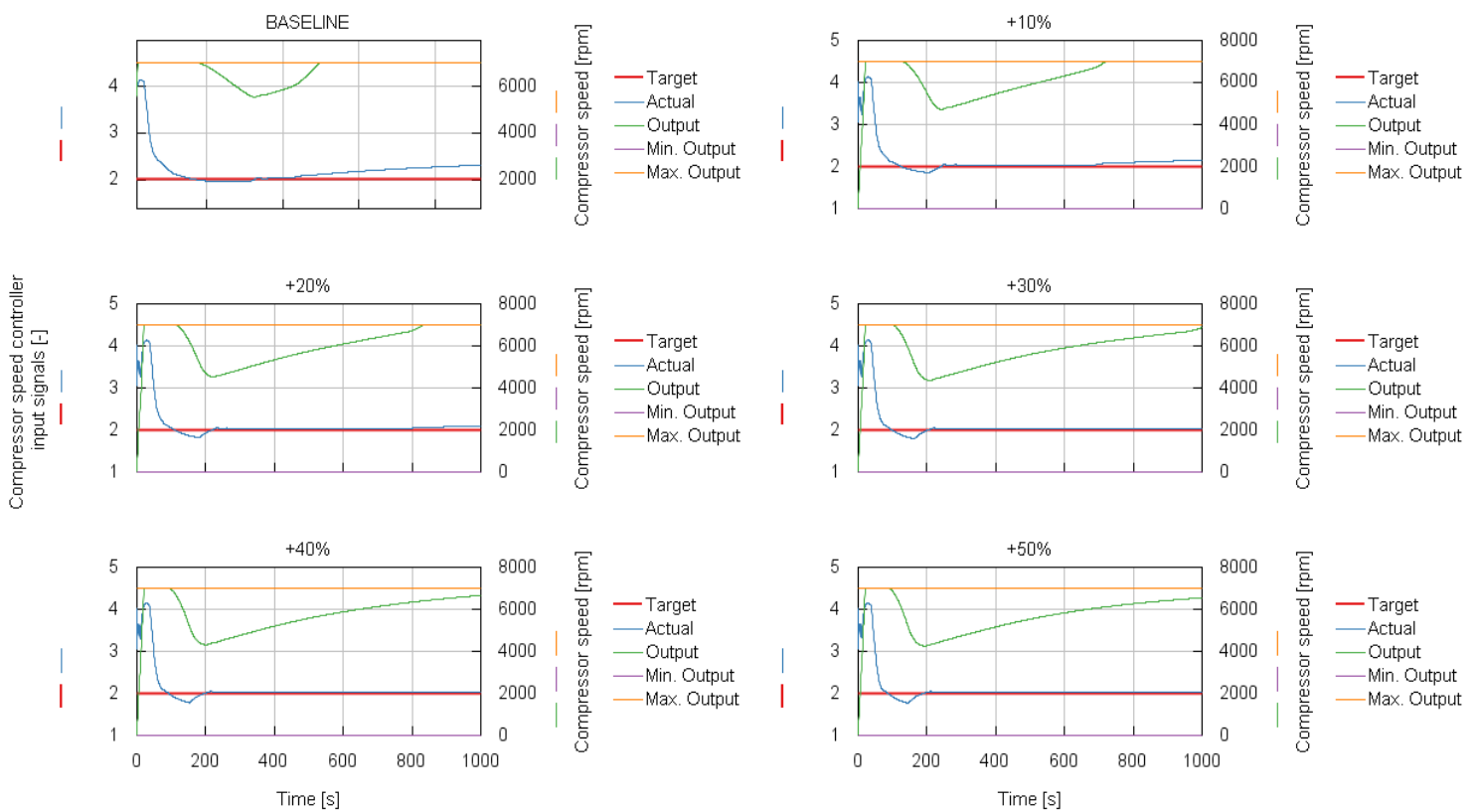


Figure 4.7 Performance summary condenser scaling

Just for reference, the same quantities plotted in *Figure 4.6* are shown in *Figure 4.7*.

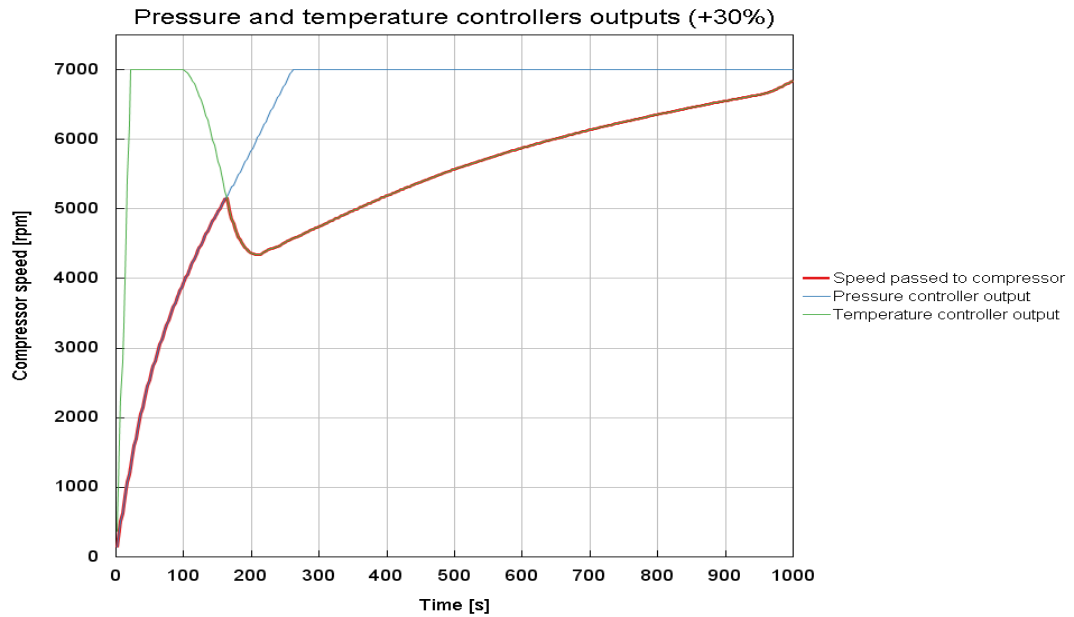


Figure 4.8 Compressor speed control (+30%)

Also from the pressure point of view, the system improves from +30% case on. Apart from the start, in which the temperature PID naturally goes for the maximum speed to reduce temperatures quickly, the compressor receives the speed needed to achieve temperature target from 150s on.

A similar analysis could be carried out for different the components of the HVAC circuit, maybe isolating the issue and acting consequently. For example, if the problem is faced in the cabin temperature target, it could be smart to scale only the cabin evaporator, or to scale only the chiller if, conversely, there is something wrong with the coolant temperature. Either way, the model could be a useful tool to select several components, also from different circuits.

4.3 Cabin heating strategy to optimize energy consumption

Differently from the cases analysed in previous sections, now the focus is shifted on the cabin heating. The battery is still being cooled down, so the heat extracted by the chiller can be released to the cabin, instead of being wasted into the environment. This is called *Heat Pump mode*, and it can be beneficial in terms of energy consumption, as it will be shown. *Figure 4.9* gives an idea of the refrigerant flow path in case heat pump mode is active.

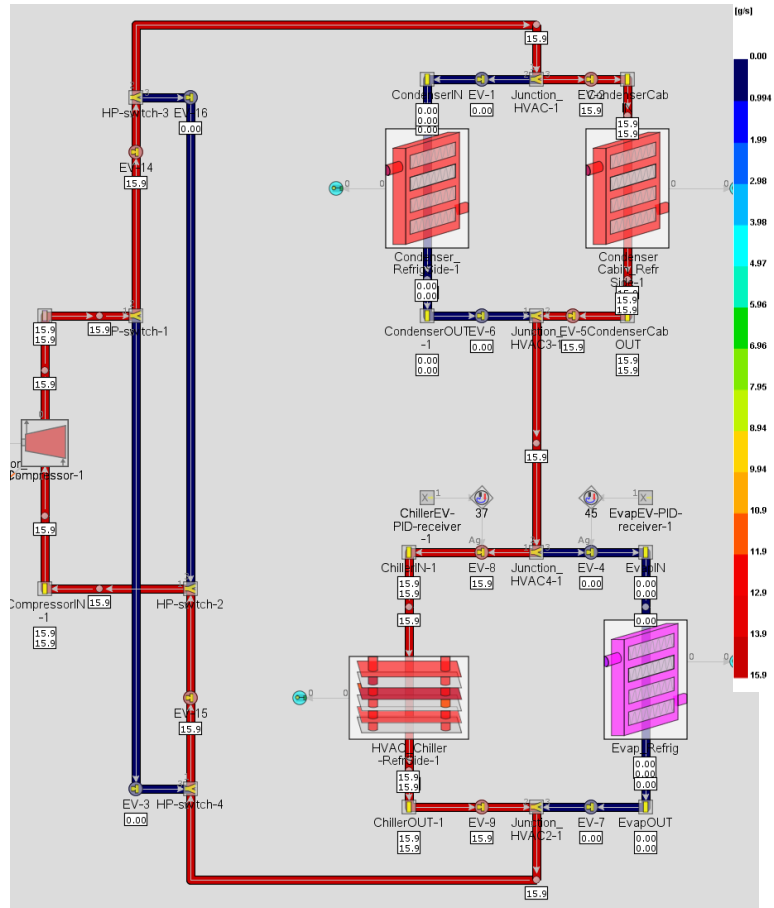


Figure 4.9 Refrigerant flow path

As the cabin is being warmed up, it is easy to understand that the flow will evaporate only in the chiller, and that the valves area controller will just pass the area needed to achieve the superheat target to *EV8*; the additional PID will be not active.

The coolant circuit layout is the same already used in *Sections 4.2* and *4.1*, no heat rejection is imposed on the motor, inverter, DC/DC and OBC thermal masses.

For what the cabin air circuit is concerned, *EV10* and *EV11* (*Figure 3.12*) will stay closed in heat pump mode, isolating the evaporator in parallel with the HVAC system. The blower is actuated at high speed, so that the quantity of generated flow rate will not bottleneck the heat exchanged in the condenser and the cabin temperature target can be achieved quickly. For this simulation, the electric cabin heater is employed, in order to control also the temperature felt by the passengers.

As a matter of fact, the purpose of this analysis is to understand whether it is more convenient from the energy consumption point of view, to heat up the cabin via heat pump mode, via electric heater or via a combination of the two. The problem of energy consumption is really debated nowadays, as the range of a BEV is one of its major weak points. Lots and lots of manufacturers strive to build electric vehicles with improved battery autonomy, achieved by improving the technology on one side, but also finding

optimized methodologies for energy utilization on the other. It is also in this prospective that the increasing complexity and costs of an HVAC system are justified.

In order to carry out the analysis, four cases have been set up, each of them having 1700W of heat rejected by the battery. The parameter that is swept is the heat introduced in the air circuit by the heater, it being 0W, 2200W, 3500W and 5000W. The cases in which the heater is active, are tested with no heat pump at all. This means that the flow condenses in the underhood heat exchanger, and that the cabin air is warmed up only by the heater. In this way, a comparison between the power consumed to reach a target temperature can be done. All the other boundary conditions include: pump and fan on the coolant circuit at high speeds (4000 rpms and 2230 rpms), 80 Km/h of vehicle velocity, initial coolant temperature at 28 °C and initial ambient and coolant temperatures at 10°C.

The controllers' targets remain the same of *Sections 4.2* and *4.1*, 10K of compressor inlet superheat and 25°C of chiller outlet coolant temperature. The target on the air temperature at evaporator outlet is not managed by the area controller anymore, since all the flow expands upstream of the chiller through *EV8*. A control strategy could be employed on the valves diverting the flow towards the condensers, *EV1* and *EV2*; however, in the studied configuration the flow goes exclusively either into the cabin condenser or the underhood one. In heat pump mode, all the energy the refrigerant receives from the battery heat rejection and the compressor is given to the cabin circuit through the cabin condenser. On the other hand, in CASE 2,3,4 it is only the heater to give energy to the cabin circuit, while the compressor is employed to cool down the battery. The monitored temperature will be the one of the cabin, considering 25°C as the requirement, so all the energy consumption calculation will be done considering the achievement of 25°C as the end of integration.

4.3.1 Energy calculation methodology and results

The power consumption of the considered configurations includes the power given to the electric heater and the one needed to activate the compressor, depending on the case. Knowing the power, the energy has to be calculated by means of an integration in time domain. For what the heater is concerned, the power spent is a constant, so the energy calculation is simply performed by multiplying the power value by the time interval. The power consumption on the compressor, on the other hand, is not constant, so an integrator block has been added to the model, taking the power trace as the input signal.

The integration intervals are considered to start from the beginning of the simulation (0s) up to the instant in which the cabin reaches 25 °C, that depends on the case. For this reason, an iterative procedure has been undertaken, running the model the first time to find the integration intervals and running it again to let the software perform the integral. *Figure 4.10* shows the intervals for each case.

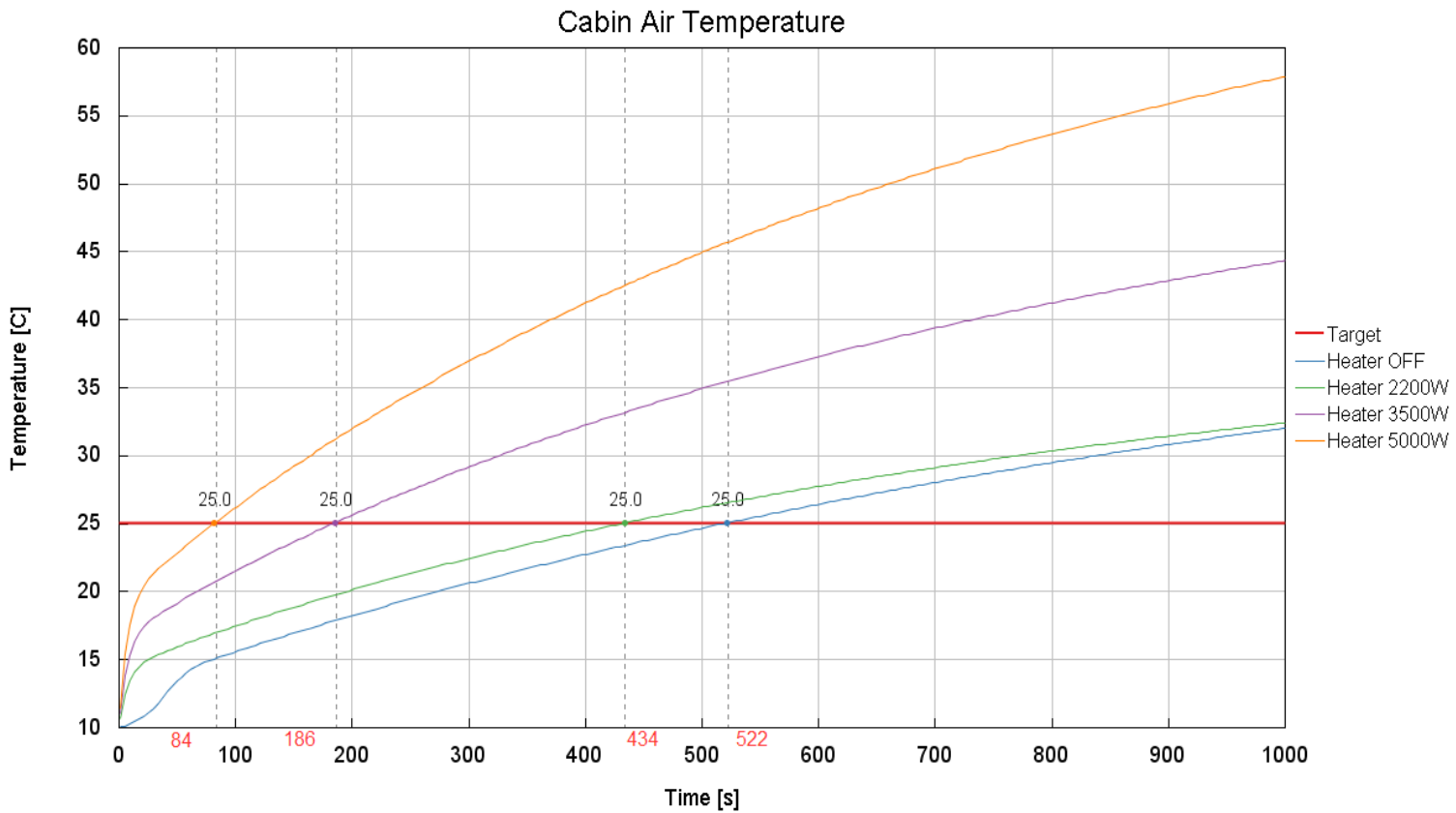


Figure 4.10 Integration intervals

Figure 4.11 summarizes the results of each case, being the energy value the one coming from GT-SUITE integration block.

As one would expect, the Heat Pump mode is the case in which the least amount of energy is spent, just a little more than 50 Wh to cool down the battery and warm the cabin up. On the negative side, 25°C are reached after almost 9 minutes, and this could be not desirable in certain situations. For CASE 2, the heater power has been chosen in order to match the mean value of the heat exchanged by the cabin condenser in CASE 1. In this way, the heat input rate given to the circuit is the same in the two cases, but the target temperature is reached more quickly, after about 7 minutes. This comes at cost of energy consumption, 265 Wh to which the compressor energy has to be summed up, since the battery still needs to be cooled down; in total the energy spent is almost 6 times higher than CASE 1, about 300 Wh. It is interesting to notice that as the power of the electric heater is increased, the energy spent drops: it becomes more than half with respect to CASE 2 when the heater is used at full capacity. This is because the cabin reaches 25 °C after only 84s at 5000W of heat input rate and so the integration interval gets a 5 times reduction. This means not only that the energy spent by the heater is lower, but also the contribution of the compressor decreases even if the power needed is the same, since among CASE 2,3 and 4 the compressor controller sees no changes.

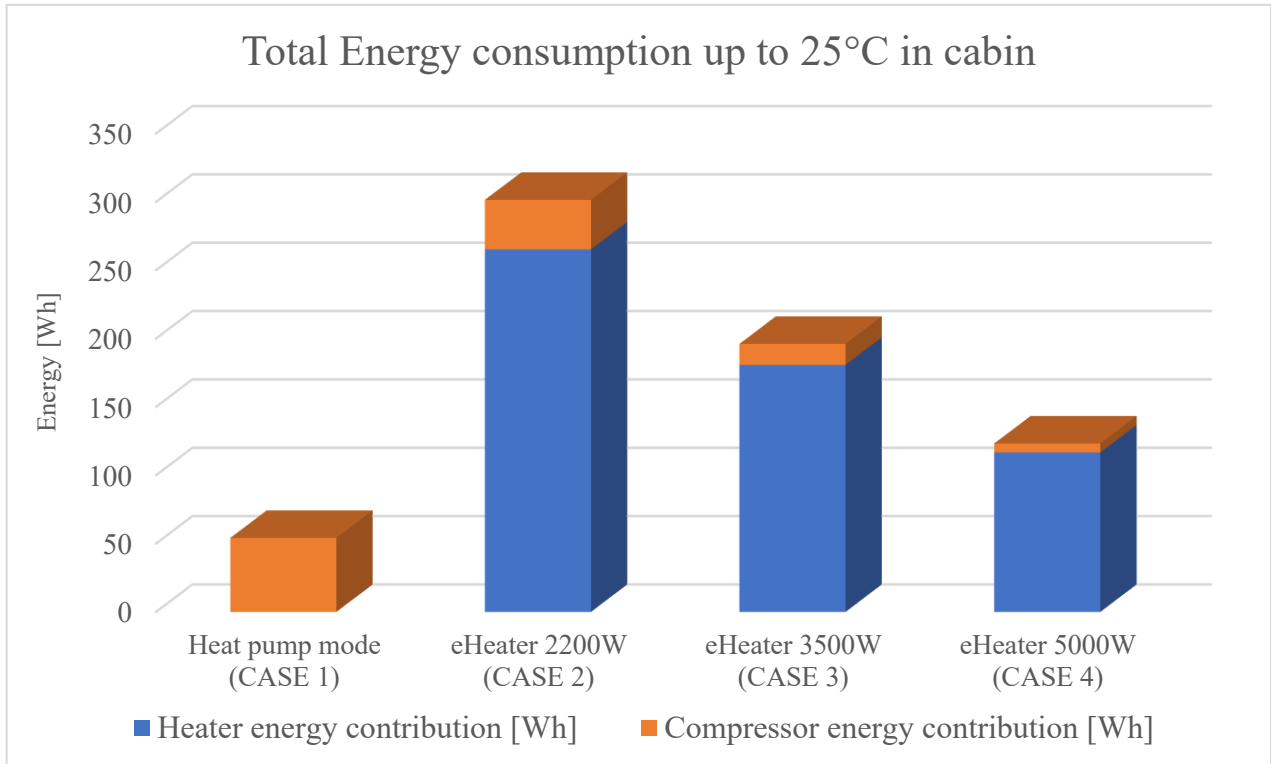


Figure 4.11 Energy calculation results

In conclusion, using the heat pump mode to heat up the cabin is without a doubt, the most convenient solution in terms of energy consumption, even if it takes some time. However, if the passengers need the target to be achieved sooner, the heater has to be switched on. In this situation, the best solution is to activate it at its maximum capabilities; an intermediate heat input rate will result in a waste of energy. To sum all up, the best strategy to follow actually depends on the specific case. For example, if the external temperatures are too low, the heater could be switched on to bring the cabin temperature up quickly in the first part of the heating process, and then the heat pump mode could be used to reach the target. However, also the battery conditions has to be taken into account. If the SOC is high enough, the system could be able to choose among the different combinations of heater/heat pump, but if it is too low, only the heat pump mode should be admissible.

Conclusions

Nowadays, the increasing strict regulations about tailpipe emissions lean the market on one side and the automotive manufacturers on the other, to look at the electrified powertrains, and specifically at BEVs after the combustion engine sales ban in 2035 approved on the 8th of June 2022, as a potential solution. Despite electric vehicles are at the moment the most feasible and immediate alternative, there is no doubt about the fact that the technology behind a pure electric vehicle has still room for improvement, being the battery autonomy one of its main limitations. For this reason, is crucial for vehicle manufacturers to have access to reliable tools to be able to simulate vehicle systems and predict their behaviour, in order to choose the best trade-offs in terms of components and control strategies.

In a BEV, the TMS is one of the most critical systems, given its high complexity and fundamental role not only in passenger comfort but also in powertrain components integrity. The integrated model that has been presented, has been built with the purpose of providing a predictive tool, useful in generic TMS simulation applications.

In *Chapter 4*, the goodness of the results has been shown, highlighting how the model can be employed to select specific components or to test different control strategies, in order to find the least energy-demanding one. As a matter of fact, after having found the main limitations of the model as it has been designed, the condenser selection procedure has been presented, successfully demonstrating how to replace the component in exam to achieve specific targets. In addition, an analysis of the energy needed to make the cabin heat up to 25 °C has been carried out, stating that the most convenient solution in terms of power consumption is to employ the heat pump mode in the HVAC system. These are really important results of the project, as they show that the developed model is versatile enough to extend the case studies to other components or to other type of analysis.

Although being generic and built taking some simplified assumptions, the TMS model is representative of a real-world BEV application and it is capable of carrying out predictive qualitative analysis. A better accuracy of the results from a numerical standpoint would be only possible with precise input and validation data referring to a specific application. Moreover, if assumptions have been made on one side, a conservative approach has been used to validate the model on the other, imposing extreme boundary conditions that in reality can be faced only for short periods of time.

In addition, further investigations on the project could regard the employment of the HVAC heat pump mode to heat up the battery, with a necessary flow path inversion thanks to solenoid valves already included in the model.

The importance of 1D simulations and models as the one built in this project help OEMs to reduce development times and costs, translating in a virtual environment analysis that otherwise could be performed only experimentally, requiring a prototype of the system at least. In addition, they allow testing in a wider range of operative

conditions, DoE and optimizations that could not be carried out in experimental classical activities.

Bibliography

- [1] Irle Roland, “Global EV sales for 2021”, EV-volumes.com, <https://www.ev-volumes.com/country/total-world-plug-in-vehicle-volumes/>, accessed 21/05/2022
- [2] Denchak Melissa, “Greenhouse effect 101”, nrde.org, <https://www.nrdc.org/stories/greenhouse-effect-101>, accessed 24/05/2022
- [3] Ritchie Hannah, “Cars, planes, trains: where do CO2 emissions from transport come from?”, ourworldindata.org, <https://ourworldindata.org/co2-emissions-from-transport>, accessed 24/05/2022
- [4] Van Hood Sam, “European Commission launches proposals to reach 55% emissions reduction by 2030”, unsdsn.org, <https://www.unsdsn.org/european-commission-launches-proposals-to-reach-55-emissions-reduction-by-2030>, accessed 24/05/2022
- [5] Clean Energy Institute, “Lithium-Ion battery”, University of Washington, <https://www.cei.washington.edu/education/science-of-solar/battery-technology/>, accessed 24/05/2022
- [6] U.S Department of energy, “Where the Energy Goes: Electric Cars”, fueleconomy.gov, <https://www.fueleconomy.gov/feg/atv-ev.shtml>, accessed 25/05/2022
- [7] Łebkowski Andrzej, “Temperature, Overcharge and Short-Circuit Studies of Batteries used in Electric Vehicles”, https://www.researchgate.net/figure/Dependence-of-internal-resistance-versus-temperature-for-lithium-based-batteries-LiFePO_fig15_316171277, doi: 10.15199/48.2017.05.13
- [8] Holcomb Brad, “ICE vs. xEV Automotive Thermal Management Simulation”, gtisoft.com, <https://www.gtisoft.com/blog-post/ice-vs-xev-automotive-thermal-management-simulation/>, accessed 25/05/2022
- [9] HellaTech World, “Car refrigerant & oil filling quantities”, <https://www.hella.com/techworld/ae/Technical/Car-air-conditioning/Car-refrigerant-oil-filling-quantities-2114/>, accessed 27/05/2022
- [10] Chowdhury, S., Leitzel, L., Zima, M., Santacesaria, M. et al., “Total Thermal Management of Battery Electric Vehicles (BEVs)”
SAE Technical Paper 2018-37-0026, 2018, doi:10.4271/2018-37-0026
- [11] Lars, “Using Tesla thermal management system parts”, evcreate.nl, <https://www.evcreate.nl/using-tesla-thermal-management-system-parts/>, accessed 29/05/2022

- [12] Darryn John, “*Tesla Model S and Model X get new heat pump, making entire lineup more efficient*”, driveteslacanada.ca, <https://driveteslacanada.ca/model-s/tesla-model-s-x-refresh-heat-pump/>, accessed 29/05/2022
- [13] Tesla Inc., “*Optimal source electric vehicle heat pump with extreme temperature heating capability and efficient thermal preconditioning*”, patent: US20190070924A1, <https://patents.google.com/patent/US20190070924A1/en?q=US20190070924A1>.
- [14] Lyngyan J, “*How does Tesla Model Y Heat Pump Work - working principles of the heat pump system and its octovalve*”, youtube.com, <https://www.youtube.com/watch?v=O19iv23An7I>, accessed 29/05/2022
- [15] Gamma Technologies, “*Flow Theory Manual*”, 2021
- [16] Gamma Technologies, “*Cooling Systems and Thermal Management Application Manual and Tutorial*”, 2021
- [17] Gamma Technologies, “*Two Phase (A/C and WHR) Applications Manual*”, 2021